

# Computational Modeling for Personalized Transcranial Electrical Stimulation: Theory, Tools, and Applications

Mo Wang<sup>1,2</sup>, Kexin Zheng<sup>1</sup>, Yiling Liu<sup>1</sup>, Huichun Luo<sup>3,4</sup>, Tifei Yuan<sup>5</sup>, Hongkai Wen<sup>2</sup>, Pengfei Wei<sup>6</sup>, and Quanying Liu<sup>1,\*</sup>

<sup>1</sup>Department of Biomedical Engineering, Southern University of Science and Technology, Shenzhen, China

<sup>2</sup>Department of Computer Science, University of Warwick, Coventry CV4 7AL, United Kingdom

<sup>3</sup>Department of Anesthesiology, Renji Hospital, Shanghai Jiao Tong University School of Medicine, Shanghai, China

<sup>4</sup>Key Laboratory of Anesthesiology (Shanghai Jiao Tong University), Ministry of Education, Shanghai, China

<sup>5</sup>Shanghai Key Laboratory of Psychotic Disorders, Brain Health Institute, National Center for Mental Disorders, Shanghai Mental Health Center, Shanghai Jiao Tong University School of Medicine and School of Psychology, Shanghai, China

<sup>6</sup>School of Biological Science and Medical Engineering, State Key Laboratory of Digital Medicine, Southeast University, Nanjing, China

\*Corresponding author: [liuqy@sustech.edu.cn](mailto:liuqy@sustech.edu.cn)

## ABSTRACT

**Objective.** Personalized transcranial electrical stimulation (tES) has gained growing attention due to the substantial inter-individual variability in brain anatomy and physiology. While previous reviews have discussed the physiological mechanisms and clinical applications of tES, there remains a critical gap in up-to-date syntheses focused on the computational modeling frameworks that enable individualized stimulation optimization. **Approach.** This review presents a comprehensive overview of recent advances in computational techniques supporting personalized tES. We systematically examine developments in forward modeling for simulating individualized electric fields, as well as inverse modeling approaches for optimizing stimulation parameters. We critically evaluate progress in head modeling pipelines, optimization algorithms, and the integration of multimodal brain data. **Main results.** Recent advances have substantially accelerated the construction of subject-specific head conductor models and expanded the landscape of optimization methods, including multi-objective optimization and brain network-informed optimization. These advances allow for dynamic and individualized stimulation planning, moving beyond empirical trial-and-error approaches. **Significance.** By integrating the latest developments in computational modeling for personalized tES, this review highlights current challenges, emerging opportunities, and future directions for achieving precision neuromodulation in both research and clinical contexts.

## 1 Introduction

Transcranial electrical stimulation (tES) is a non-invasive neuromodulation technique that delivers low-intensity electrical currents to the scalp with the objective of modulating brain activity. Compared to invasive techniques such as deep brain stimulation (DBS), tES offers great advantages in safety, accessibility, and cost-effectiveness [1, 2]. Accumulating evidence indicates that tES can modulate neural oscillations and cortical excitability, thereby influencing a range of cognitive functions and behaviors [3, 4, 5, 6]. As such, tES has been widely applied as both a research tool to probe causal brain-behavior relationships and a therapeutic intervention for neurological and psychiatric conditions [7, 8, 9, 10, 11, 12].

The efficacy of tES is influenced by various factors, including electric field strength and orientation, stimulation frequency, waveform characteristics, and even the ongoing brain state [1, 3, 13]. Multiple tES modalities have been developed, including transcranial direct current stimulation (tDCS) [14, 15], transcranial alternating current stimulation

(tACS) [16, 17], transcranial random noise stimulation (tRNS) [18], intersectional short pulse stimulation (ISP) [19], and temporal interference stimulation (TIS) [20, 21, 22]. Each modality offers distinct mechanisms of action and application potentials, providing researchers and clinicians with versatile tools for neuromodulation.

A growing body of research has highlighted the substantial inter-individual variability in neuroanatomy and neurophysiology, prompting increasing interest in personalized tES strategies [23, 24, 25, 22]. While several earlier works touched upon personalization in tES [26, 27, 28], most reviews have emphasized physiological mechanisms or clinical efficacy [3, 29, 30], with comparatively less attention paid to the computational frameworks that support individualized targeting and optimization. Given that computational models now play a central role not only in estimating electric field distributions but also in systematically optimizing stimulation parameters, a focused synthesis of these advances is urgently needed.

Computational models in tES serve a dual role: forward simulation (Fig.1 A-E) and inverse optimization (Fig.1 F-I). Forward modeling, often referred to as head volume conduction modeling, predicts the spatial distribution of electric fields induced within the brain during stimulation. This capability is essential for mechanistically understanding how tES modulates neural activity [31]. Traditional forward models often rely on standardized anatomical templates such as MNI152 [32, 33] or ICBM152 [34]. However, substantial inter-individual variability in head anatomy, tissue conductivity, and cerebrospinal fluid distribution can lead to marked differences in electric field profiles even under identical stimulation conditions [35, 36, 37]. Consequently, constructing subject-specific head models from individual MRI scans has become critical for achieving accurate simulations. Recent advances in neuroimaging acquisition and segmentation pipelines have dramatically reduced the time required to build individualized head models, paving the way for broader clinical and research applications.

Alongside the evolution of modeling techniques, tES hardware has also advanced—from simple two-electrode setups to complex multi-electrode arrays—substantially expanding the parameter space for stimulation configuration. Manual montage design or simple forward simulation is often insufficient to identify optimal stimulation strategies in this high-dimensional space [38]. Inverse optimization methods have thus emerged as essential tools, integrating personalized forward models with optimization algorithms to systematically determine stimulation parameters that maximize efficacy, enhance target specificity, and minimize unintended effects. Optimization techniques explored in the field include exhaustive search [39, 40], quadratic programming [41], gradient-based methods [42], and heuristic algorithms such as genetic optimization [22, 43]. Critical factors in inverse modeling include the definition of biologically meaningful objective functions, adherence to safety constraints, and accommodation of hardware limitations. Moreover, integrating multimodal information, such as functional or structural connectivity data, offers opportunities for network-informed dynamic stimulation designs. These recent advances and their implications for future personalized tES development are systematically discussed in this review.

This review aims to fill this gap by providing a comprehensive and structured overview of computational modeling approaches for personalized tES. Specifically, we examine forward modeling (used to predict electric field distributions) in Section 2 and inverse optimization (used to tailor stimulation strategies) in Section 3, and discuss how recent advances in neuroimaging, numerical solvers, optimization algorithms, and multimodal data integration are shaping the future of precision neuromodulation in Section 4. Finally, we discuss the current limitations of computational modeling in tES and outline promising future directions for research and application.

## 2 Forward modeling for personalized tES

Forward modeling, also known as volume conduction modeling, plays a fundamental role in simulating the distribution of electric fields generated by (Table 1) (Fig.1 A-E). The earliest modeling work employed simplified spherical head models, which approximated the human head as three nested concentric spheres representing the scalp, skull, and brain, respectively. Despite their simplicity, these models effectively captured key aspects of electric field distribution and demonstrated reasonable agreement with experimental measurements [44]. As the field progressed and the demand for realistic head models increased, researchers began incorporating real anatomical data into head conductivity models using MRI-based imaging. The construction of realistic forward models typically involves several major steps: tissue segmentation, mesh generation, and electric field simulation. In the early stages, constructing individualized models was time-consuming and labor-intensive, prompting the widespread use of standardized templates for forward modeling. Among the most prominent templates are the MNI152 head model [32, 33], derived from the average of 152 anatomical scans, and the New York Head Model introduced by Huang et al.[45], a finite element method (FEM)-based model built upon the ICBM152 template. These resources have significantly advanced large-scale and reproducible tES research [46, 47, 48]. Recent advances in neuroimaging pipelines and high-performance computing have made the construction of subject-specific head models increasingly practical. Personalized head models can

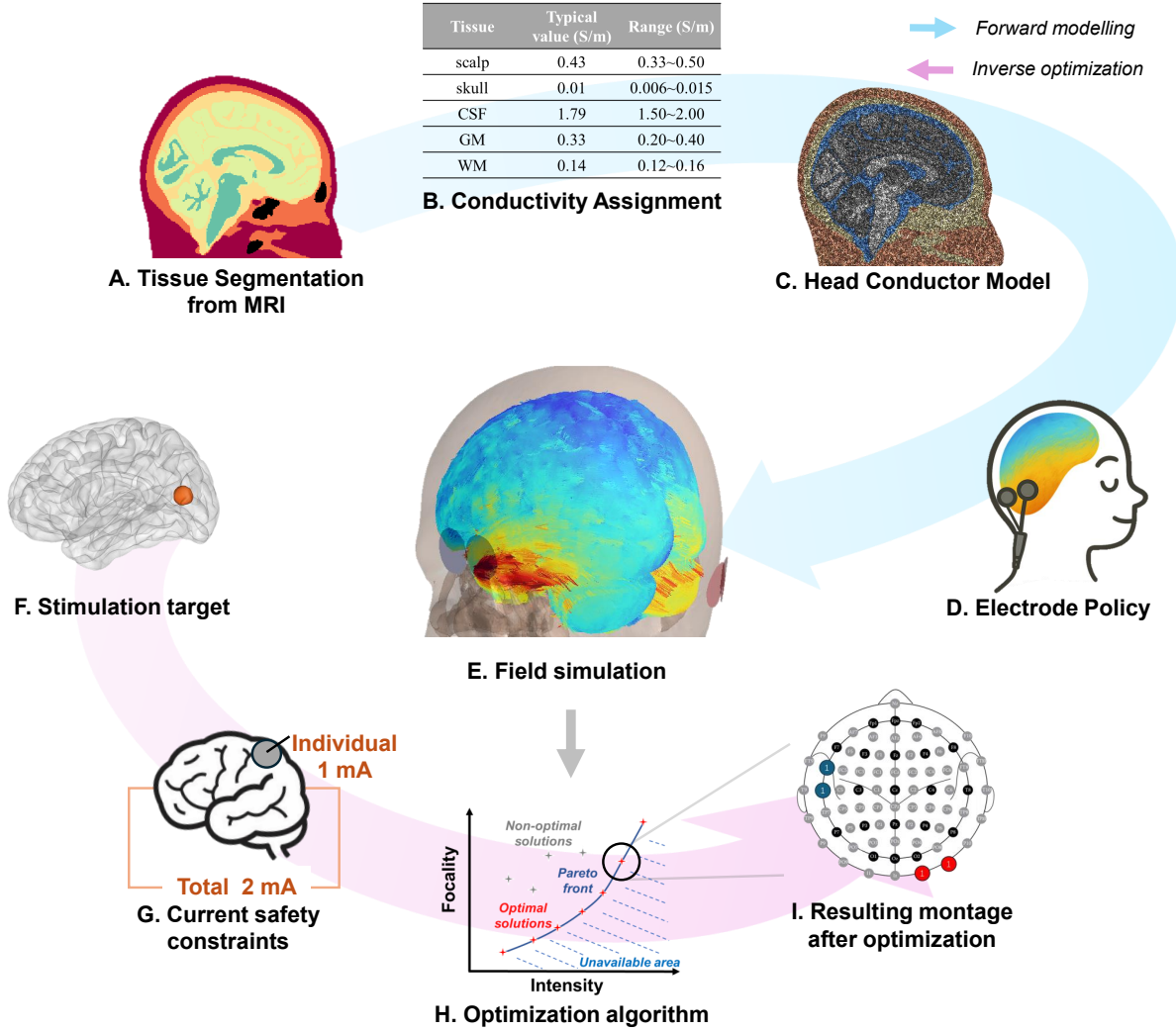


Figure 1: Overview of the forward modeling and inverse optimization for personalized tES. (A) The construction of forward models for personalized computational simulations begins with tissue segmentation from MRI data. (B) Conductivity values are assigned to each segmented tissue type to generate an individualized computational model. (C) Head conductor model is generated by mesh generation and numerical methods. (D) Virtual electrodes are then positioned on the model, and current is applied according to the predefined stimulation protocol. (E) The electric field distribution is simulated by solving the current flow within the head model. The stimulation montage is optimized based on the electric field simulation results from the forward model. (F) The stimulation target is first identified, followed by (G) verifying current safety constraints. (H) An optimization algorithm is then applied to the model to determine optimal stimulation parameters. (I) Based on the optimization results, a stimulation montage is applied to the personalized tES for the subject.

now be generated from individual MRI within a few hours, often fully automatically, thus enabling individualized simulation of electric fields prior to tES intervention.

In the following sections, we review the formulation and evolution of forward modeling approaches for personalized tES, from early spherical models to anatomically realistic, individualized simulations. This progression illustrates the field's continuous efforts to improve the accuracy and targeting precision of tES through increasingly advanced computational tools.

## 2.1 Tissue Segmentation, Electrode Co-registration, Mesh Generation and Numerical Methods

The construction of computational head models begins with tissue segmentation, a process that extracts anatomical structures from medical imaging data such as MRI or computed tomography (CT) scans (Fig. 1 A).

Segmentation involves delineating key tissues relevant to electrical conductivity, including the scalp, skull, cerebrospinal fluid (CSF), gray matter (GM), and white matter (WM). Conductivity values derived from empirical measurements are assigned to segmented tissues to enable electric field distribution calculations (Fig. 1 B). Accurate segmentation is the first critical step toward effective modeling. Segmentation quality is commonly assessed using metrics such as the Dice coefficient and the modified Hausdorff distance, each providing complementary insights. The Dice coefficient measures the similarity between two sets, by computing the ratio of twice their intersection to the sum of their cardinalities. While the Dice coefficient effectively captures the overlap of large voxel clusters, it may overlook subtle discrepancies along region boundaries. To address this limitation, the modified Hausdorff distance [49] is often employed. It calculates the average of two directed Hausdorff distances, where each directed distance represents the maximum deviation from a point in one set to its nearest neighbor in the other. By focusing on boundary dissimilarities, the modified Hausdorff distance offers a finer-grained evaluation of segmentation accuracy. In practice, better segmentation results are indicated by a higher Dice coefficient and a lower modified Hausdorff distance.

Following segmentation, electrode co-registration is performed to accurately align stimulation electrodes with the individual's anatomical structures. This step ensures that electrode positions correspond to the same spatial coordinates as the segmented tissues. The procedure is analogous to electrode registration techniques used in EEG studies, typically employing standard scalp landmarks to maintain consistent positioning relative to brain anatomy.

The next step is mesh generation for model construction, where the segmented head tissues are discretized into a network of nodes and elements to enable numerical simulations (Fig. 1 C). High-quality meshes are critical for accurately modeling electric field distributions and optimizing computational efficiency. The mesh resolution directly affects the model's ability to capture the complex geometry of the head and faithfully replicate the spatial patterns of electric fields during tES. The choice of meshing methods depends on the numerical methods employed. In computational modeling, a mesh is a crucial bridge connecting physical problems to mathematical models. Different numerical methods have distinct requirements and approaches for meshing.

The Finite Element Method (FEM) is the most widely adopted [50, 51], owing to its flexibility in handling complex geometries and heterogeneous, anisotropic conductivity distributions [52]. FEM discretizes the volume into small elements, enabling high-fidelity approximations of electric fields in intricate anatomical structures. An alternative approach is the Boundary Element Method (BEM), which simplifies the problem by meshing only the boundaries between tissues [53, 54]. By reducing the problem dimensionality, BEM substantially lowers computational demands. However, its applicability is limited in cases involving significant conductivity inhomogeneity or anisotropy [55, 56]. Despite these challenges, recent methodological advances have improved BEM's robustness for tES applications [57, 58]. The Finite Difference Method (FDM) presents another option, discretizing the domain on structured grids. While FDM is conceptually simple and computationally efficient for regular geometries, it struggles with irregular anatomical boundaries and spatially varying conductivities, which can compromise simulation accuracy [59].

## 2.2 Finite Element Method for Electrical Field Simulation

The FEM, due to its flexibility, is well-suited for handling complex geometries and is most commonly used for modeling and solving the electric field distribution within the brain. Here, we will use the FEM as an example for a detailed introduction. Once the whole head mesh model is generated, the accuracy of these simulations critically depends on the quality of the preceding tissue segmentation and mesh generation steps (Fig. 1 D). The meshed head model incorporates the spatial distribution of conductivity across different tissues, and the electric field simulation is governed by Laplace's equation (Fig. 1 E). Assuming the absence of net current sources or sinks within the volume, the divergence of the current density ( $J$ ) vanishes. When external currents are applied through electrodes placed on the scalp, the resulting potential distribution ( $V$ ) within the head can be computed by solving the following form of

Laplace's equation [60]:

$$\nabla \cdot J = \nabla \cdot (\sigma E) = -\nabla \cdot (\sigma \nabla V) = 0, \quad (1)$$

where  $\sigma$  denotes the electrical conductivity of the tissue. Conductivity is typically assumed to be isotropic—identical in all directions—but can be extended to anisotropic models, as discussed in Section 4.

A unique solution to Laplace's equation requires appropriate boundary conditions. In tES simulations, both Neumann and Dirichlet boundary conditions are commonly employed. For instance, the potential from the electrodes, denoted as  $V_0$ , which is determined by factors such as the electrode material, size, and current source, can be applied using the Dirichlet boundary condition:

$$V = V_0, \quad (2)$$

After assembling the global matrix and applying the boundary conditions, the system is solved numerically to obtain the distribution of the electric field. To efficiently compute the potential distribution, open-source solvers such as getDP [61] can be utilized.

Table 1: Head model (volume conduction model)

Reference	Meshing Methods	Models
Miranda P C, et al. (2006). Clinical neurophysiology [44]	FEM	Spherical Head Model
Wagner T A, et al. (2004). IEEE Transactions on Biomedical Engineering [51]	FEM	Realistic Human Head Model
Datta A, et al. (2009). Brain stimulation [62]	FEM	Realistic Human Head Model
Rampersad S M, et al. (2014). IEEE Transactions on Neural Systems and Rehabilitation Engineering [63]	FEM	Realistic Human Head Model
Fuchs M, et al. (2002). Clinical neurophysiology [54]	BEM	Realistic Human Head Model
Susnjara A, et al. (2019). International Conference on Software, Telecommunications and Computer Networks (SoftCOM) [57]	BEM	Realistic Human Head Model
Šušnjara A, et al. (2022). Engineering Analysis with Boundary Elements [58]	BEM	Realistic Human Head Model
Magsood, H., et al. (2021). Materials Science and Engineering [64]	FDM	Realistic Human Head Model

Continued on next page.

### 2.3 Simulating electrical field distribution induced by tES

After obtaining the electric field in a single direction by anode and cathode, according to [66], the averaged electric field norm of tDCS can be formulated as Eq. (3).

$$E = \sqrt{w_x E_x^2 + w_y E_y^2 + w_z E_z^2}, \quad (3)$$

where  $x$ ,  $y$  and  $z$  represent three orthogonal directions, and  $w_x$ ,  $w_y$ , and  $w_z$  denote the weights assigned to the respective orthogonal directions. And because tACS usually has low frequency, a quasi-static approximation can be employed to simulate it. In most cases, we can derive the electric field at peak currents from computational models. The temporal variations of the current merely scale the field without altering its distribution within the brain. When multiple channels are out of phase, simulations should be based on temporal dynamics. Saturnino et al. modeled several in-phase and anti-phase tACS scenarios, finding that they produced complex differences in temporospatial stimulation patterns [67].

tTIS employs a distinct mechanism to stimulate the brain. Two-pair tTIS utilizes two pairs of electrodes, while HD-tTIS employs an array of electrodes for stimulation [68]. Both types of stimulation are designed to stimulate the brain by the low frequency envelope formed by high frequency current. The effect of tTIS can be evaluated by the modulation depth, which is defined as the difference between the maximal and minimal value of the envelope. As models disregard the possible effects of high-frequency stimulation on neurons, they calculate the distinct frequency electric field in the same manner as tACS (Eq. (1), (2)). The envelope field with the desired direction can be calculated by the formula proposed by Grossman et al. [20], shown in Eq. (4).

$$|\vec{E}(\vec{r})| = |(\vec{E}_1(\vec{r}) + \vec{E}_2(\vec{r})) \cdot (\vec{n})| - |(\vec{E}_1(\vec{r}) - \vec{E}_2(\vec{r})) \cdot (\vec{n})|, \quad (4)$$

where  $\vec{E}_1(\vec{r})$  and  $\vec{E}_2(\vec{r})$  are the first and second distinct fields at the location  $\vec{r}$  and  $\vec{n}$  is an unit vector along the desired direction. And Huang et al. provided a comprehensive analysis of the equations governing various forms of tTIS [69, 68]. They showed the formulae for the modulation depth along the maximum direction. It is straightforward to find that Eq. (4) is maximized if and only if  $\vec{n}$  falls onto the plane spanned by  $\vec{E}_1$  and  $\vec{E}_2$ . Under such premise, the maximal modulation depth equation can be formulated as follows.

$$|\vec{E}| = 2 \max_{\alpha} \min(|\vec{E}_1| \cos \alpha, |\vec{E}_2| \cos(\alpha - \phi)) \quad (5)$$

where  $\phi$  is the angle spanned by  $\vec{E}_1$  and  $\vec{E}_2$ , and  $\alpha$  is the angle between  $\vec{E}_1$  and the projection of  $\vec{n}$  on that plane. 1D-search over  $\alpha \in [0, 2\pi)$  can be performed to find the maximal modulation where  $\vec{E}_1$ ,  $\vec{E}_2$  and  $\phi$  are known from computational model. In addition, they proved by the equations that a conventional TES approach (tACS and tDCS) can always be made to reach stronger modulation depth than tTIS regardless of which field orientation one considers.

### 2.4 Software for constructing personalized head models

General-purpose FEM software, such as COMSOL Multiphysics (COMSOL, Inc., Burlington, MA), can be utilized for constructing personalized head models. These platforms offer flexible environments for steady-state electrical current simulations, featuring user-friendly interfaces that allow users to define material properties, boundary conditions, and solver settings. Once the model is configured with appropriate tissue conductivities and boundary specifications, the underlying physical equations can be efficiently solved.

In addition to general FEM platforms, several software packages have been specifically developed for brain stimulation modeling, providing end-to-end solutions for the construction and simulation of personalized head models (see Table 2). These include ROAST [70], SimNIBS [66, 71], SCIRun [72], COMETS [73], and SimBio [74]. Among these, ROAST and SimNIBS are the most widely adopted open-source tools in the field. In the following sections,

we introduce the computational frameworks underpinning ROAST and SimNIBS, and provide a comparative analysis highlighting their respective strengths, limitations, and suitable application scenarios.

**SimNIBS 2.1:** SimNIBS 2.1 provides two distinct pipelines for head segmentation and mesh generation: *headreco* and *mri2mesh*. Among these, *headreco* is recognized for its significantly faster processing speed, typically completing within 2 hours, while *mri2mesh* requires approximately 10 hours to achieve comparable results, according to the official documentation. The *mri2mesh* pipeline relies on FreeSurfer [75] (version 5.3.0 or newer) and FSL [76] (version 5.0.5 or newer), and thus is not compatible with the Windows operating system. In contrast, *headreco* utilizes voxel segmentations generated by SPM12 combined with morphological operations, and can run seamlessly across Windows, Linux, and macOS platforms. Notably, *headreco* supports the use of CAT12 to reconstruct the mid-thickness gray matter (GM) surface, enabling more anatomically accurate individualized head models. Both *headreco* and *mri2mesh* share a similar approach to converting voxel segmentations into volume meshes, as described in Windhoff et al. [77].

In terms of segmentation accuracy, MRI-based evaluations reveal that *headreco* and *mri2mesh* achieve comparable performance in Dice similarity scores. However, *headreco* demonstrates a lower Hausdorff distance, indicating more precise delineation of the skull boundaries. Additionally, incorporating a T2-weighted (T2w) image into the segmentation pipeline generally improves the robustness and quality of results [78, 79, 80]. Specifically, the inclusion of T2w images reduces inter-subject variability and mitigates instances of gross segmentation errors, due to the enhanced contrast between skull and cerebrospinal fluid (CSF) compared to T1-weighted (T1w) images.

Regarding mesh quality, both *headreco* (with CAT12 integration) and *mri2mesh* produce head meshes of comparable geometric fidelity. The quality of finite element meshes is typically assessed using metrics such as the Aspect Ratio ( $\rho$ ), Volume-to-Edge Ratio ( $\eta$ ), and Volume-to-Surface Ratio ( $\tau$ ), where lower values indicate more regular and well-shaped tetrahedra. Comparative analyses reveal no substantial differences in mesh quality between the two pipelines, likely attributable to their similar surface generation and volume meshing strategies. Interestingly, finer anatomical modeling of cortical folding, especially detailed sulcal structures, slightly increases the occurrence of lower-quality tetrahedra. This effect is observed across segmentation methods, whether employing FSL BET2 and FreeSurfer for *mri2mesh*, or SPM12 and CAT12 for *headreco*.

**SimNIBS 4:** In the latest versions of SimNIBS, the *CHARM* pipeline has replaced earlier tools such as *headreco* and *mri2mesh*, offering improved head segmentation performance. *CHARM* automatically segments fifteen different head tissues from magnetic resonance (MR) images. A key advantage of *CHARM* is its robustness to variability in input scans, allowing it to be applied directly to clinical or research data acquired using different scanners, sequences, or imaging protocols. Comparative evaluations using Dice coefficient and modified Hausdorff distance metrics demonstrate that *CHARM* outperforms *headreco* and *ROAST* in simplified segmentation tasks involving the five primary head tissue classes. Moreover, *CHARM* achieves consistently high segmentation accuracy across all fifteen tissue types, with higher performance observed for larger anatomical structures and slightly lower accuracy for smaller structures. Importantly, *CHARM* maintains robust segmentation quality even on lower-quality clinical datasets, highlighting its practical applicability across a wide range of imaging conditions.

**ROAST:** ROAST performs head segmentation by leveraging SPM12, similar to *headreco*, supplemented with additional post-processing operations. After obtaining the segmentation, ROAST employs *Iso2mesh* [81], a free MATLAB/Octave-based toolbox for mesh generation and processing, to create tetrahedral meshes. *Iso2mesh* is capable of generating meshes from surfaces as well as from 3D binary or grayscale volumetric images such as segmented MRI or CT scans. When comparing automated segmentation results to manual annotations, ROAST demonstrates superior performance in segmenting WM, GM, and CSF compared to *headreco* with CAT12. It shows comparable performance to *headreco* for skull and air segmentations but exhibits limitations in accurately delineating the scalp region. Additionally, *mri2mesh* performs worse than *headreco* in terms of absolute volumetric segmentation differences across multiple tissue types, further underscoring the relative advantages of ROAST and *headreco*.

Table 2: Software for forward modeling and inverse optimization. ( Only display optimization methods with official implementation, see Section 3.2 for more detailed information )

Method	Forward Modeling / Inverse Optimization	Website
--------	--	---------

Continued on next page.

SimNIBS [82]	Both	<a href="https://simnibs.github.io/simnibs/build/html/index.html">https://simnibs.github.io/simnibs/build/html/index.html</a>
ROAST [70]	Both	<a href="https://github.com/andypotatohy/roast">https://github.com/andypotatohy/roast</a>
FreeSurfer [75]	Modeling	<a href="https://surfer.nmr.mgh.harvard.edu/">https://surfer.nmr.mgh.harvard.edu/</a>
Brainstorm [83]	Modeling	<a href="https://neuroimage.usc.edu/brainstorm/">https://neuroimage.usc.edu/brainstorm/</a>
DUNEuro [84]	Modeling	<a href="https://www.medizin.uni-muenster.de/duneuro/forschung.html">https://www.medizin.uni-muenster.de/duneuro/forschung.html</a>
Iso2mesh [81]	Modeling	<a href="https://iso2mesh.sourceforge.net/cgi-bin/index.cgi">https://iso2mesh.sourceforge.net/cgi-bin/index.cgi</a>
SCIRun [72]	Modeling	<a href="https://sci.utah.edu/software/scirun.html">https://sci.utah.edu/software/scirun.html</a>
COMETS [73]	Modeling	<a href="http://cone.hanyang.ac.kr/bbs/page.php?pa_id=detail6">http://cone.hanyang.ac.kr/bbs/page.php?pa_id=detail6</a>
SimBio [73]	Modeling	<a href="https://simbio.com/">https://simbio.com/</a>
Neurophet tES LAB [85]	Modeling	<a href="https://brainbox-neuro.com/products/neurophet-tes-lab">https://brainbox-neuro.com/products/neurophet-tes-lab</a>
COMSOL [86]	Modeling	<a href="https://www.comsol.com">https://www.comsol.com</a>
Genetic Algorithm [87]	Optimization	<a href="https://zenodo.org/records/5907212">https://zenodo.org/records/5907212</a>
MOVEA [22]	Optimization	<a href="https://github.com/ncclab-sustech/MOVEA">https://github.com/ncclab-sustech/MOVEA</a>

## 2.5 Application for forward modeling

Forward modeling has proven to be an effective approach for simulating current conduction within the brain and is widely employed in various research domains [12, 88, 89, 90]. The primary applications of forward modeling in research involve targeted electric field simulations and the investigation of neuromodulatory mechanisms (see Table 3). Targeted simulations are particularly useful as validation tools before conducting experiments. Many studies utilize open-source head models to compute electric field distributions prior to experimentation, with the goal of assessing whether the stimulation paradigm effectively targets the intended brain regions.

For instance, Luo et al. assessed influence of tACS on the hippocampus and amygdala using real sEEG signals and used SimNIBS to simulate the effects of it. They found that a low-intensity electric field could modulate the activity of deep brain regions [91]. Dondé et al. employed ROAST v3.0 to simulate the electric field induced by tRNS over the left frontotemporal lobe, validating the modulatory effects of high-frequency tRNS in patients with schizophrenia [92]. Similarly, Lewis et al. used SimNIBS to simulate the impact of tDCS on the human blood-brain barrier permeability, ensuring accurate targeting of the current [93]. Beyond using generic models, customized forward models have also been developed to address specific scenarios. For example, Sun et al. investigated the therapeutic potential of tDCS for cortical lesions resulting from decompressive craniectomy (DC). They constructed a finite element head model that included a 12 cm hole at the top of the skull to simulate the surgical imprints [94]. In another study, Breitling et al. created a multimodal head model of a 13-year-old boy using SCIRun, ensuring that the model's age-specificity aligned with the corresponding subjects [95].

In addition to targeted simulations, forward modeling is extensively used to analyze neuromodulatory mechanisms. For example, Laakso et al. utilized a generic model to compute current pathways and demonstrated that retinal phosphene could be induced by current [96]. Personalized forward models are increasingly being adopted to simulate more realistic head conditions. This approach involves gathering MRI data from subjects to generate individualized models. Hamajima et al., for instance, used MRI data from 18 healthy subjects to construct forward models for analyzing the effects of tDCS montage-induced polarity changes in lower limb motor regions [97]. In another investigation, Lu et al. developed forward models for healthy older adults and those with mild cognitive impairment (MCI) to simulate the impact of scalp-to-cortex distance on tDCS-induced electric fields [98]. Additionally, Uenishi et al. simulated electric fields induced by prefrontal tDCS in individuals with mood disorders and schizophrenia, finding that the electrophysiological response to stimuli was diminished in those with schizophrenia [99].

Table 3: Applications for forward modeling

Reference	Computational Modeling	Report Findings
Dondé, C., et al. (2024). Asian journal of psychiatry [92]	ROAST	hf-tRNS could disrupt the test-retest learning effect in the tone-matching task in individuals with schizophrenia.
Yoon MJ, et al. (2024). Science Report [100]	Neurophet tES LAB	Optimized tDCS afforded a higher electric field in the target of a stroke patient compared to conventional tDCS.
Lewis, A., et al. (2023). Neuromodulation : journal of the International Neuromodulation Society [93]	SimNIBS	Although the effects of tDCS were not significant, increases in salivary S100B after a fatiguing cycling task may indicate exercise-induced changes in BBB permeability.
Hamajima H, et al. (2023). Clinical Neurophysiology [97]	FreeSurfer	Proper montage selection allows reaching deeper regions of the lower-limb motor area with uniform polarization.
Sadeghiahassanabadi F, et al. (2022). Journal of Neural Engineering [101]	SimNIBS	The jaw montage is an optimal choice for maximizing cerebellar stimulation while minimizing unwanted side effects.
Nandi et al. (2022). Brain stimulation [102]	SimNIBS	The electric field strength calculated by simulation model correlates with a decrease in GABA in the motor cortex.
VanHoornweder et al. (2022). Journal of Neural Engineering [103]	SimNIBS	Analyzed the impact of individualized versus fixed intensity tES on E-field strength variability.
Uenishi S, et al. (2022). Psychiatry Research: Neuroimaging [99]	SimNIBS	Attenuated electrophysiological response to transcranial direct current stimulation to the prefrontal cortex in patients with schizophrenia.

Continued on next page.

Sun W, et al. (2021). Journal of International Medical Research [94]	MIMICS	A guideline for selecting current and electrode montage settings when performing tDCS on patients after DC.
Lu, H., et al. (2021). Journal of neuroengineering and rehabilitation [98]	ROAST	Ageing has a prominent, but differential effect on the region-specific SCD and cortical features in older adults with cognitive impairments.
Kasten et al. (2019). Nature Communications [104]	ROAST	Integrating electric field modeling and neuroimaging to explain inter-individual variability of tACS effects.
Nissim et al. (2019). Frontiers in Aging Neuroscience [105]	ROAST	Calculating the field distribution by computational model.
Saturnino et al. (2017). NeuroImage [106]	SimNIBS	Providing a framework for selective in- and anti-phase TACS of two cortical areas by multiple montages.
Bchinger et al. (2017). The Journal of Neuroscience [17]	SimNIBS	Assessing whether two stimulation paradigms caused comparable effects by simulation model.
Huang et al. (2017). Brain Stimulation [2]	SimNIBS	Measured electric potentials intracranially in ten epilepsy patients and estimated electric fields across the entire brain by leveraging calibrated current-flow models.
Breitling, C., et al. (2016). Frontiers in cellular neuroscience [95]	SCIRun5	These results suggest that anodal tDCS of the right inferior frontal gyrus could improve interference control in patients with ADHD.
Alekseichuk et al. (2016). Current Biology [107]	SimNIBS	The anatomical target was validated by simulating the applied electric field.
Laakso, I., et al. (2013). Journal of neural [96]	The Duke Model [108]	The interference from retinal phosphenes needs to be considered in the design of tACS experiments.

### 3 Inverse Optimization for personalized tES

Once the volume conduction model is successfully constructed, a significant concern arises regarding individual variations in tES. In tDCS, due to anatomical differences among individuals, the resulting brain electric field can vary

when the same current was administered [109]. While personalized dosing control can mitigate variations in electric field strength reaching the intended target [110], anatomical variability also presents challenges in determining optimal electrode configurations [35]. Furthermore, tTIS has proven its capacity for achieving focal stimulation [22, 69]. However, the stimulation strategy becomes increasingly complex due to the sophisticated mechanism inherent in tTIS applications [20, 21, 22, 69, 111]. The optimal positioning, size, and spacing of electrodes can significantly amplify the electric field strength within the targeted stimulation zone [112] (Fig. 1 F-I).

### 3.1 Formulation of tES optimization problem

Forward modeling enables the estimation of electric field distributions under a given electrode configuration. Based on the simulation results, the effectiveness of stimulation at specific targets can be evaluated (Fig. 1 F). We can use algorithms to identify the optimal configuration for specific targets (Fig. 1 H). The input of the algorithms are objective functions and leadfield matrix. The objective functions incorporate information regarding the target and constraints. The leadfield matrix, or gain matrix, is a matrix that encapsulates the relationship between the stimulation injected at the scalp and the resulting electrical fields in the brain [60]. This matrix is obtained by sequentially applying a unit current through each candidate electrode. Each element of the matrix represents the electrical field in the corresponding area under a given stimulation. By leadfield matrix, we don't need to run the forward model for each potential configuration, significantly reducing the time cost. The electrical field can be calculated by Eq. (6)

$$E = s \cdot L \quad (6)$$

where  $s$  represents the index of the activation electrode and the corresponding current intensity, and  $L$  denotes the leadfield matrix. The leadfield matrix typically encompasses three dimensions: the electrical channel, mesh volume, and orthogonal direction. The goal of optimization is to maximize or minimize the objective functions, subjecting to constraints, as shown in Eq. (7).

$$\begin{array}{ll} \min / \max & \text{Objective function} \\ \text{s.t.} & \text{constraints} \end{array} \quad (7)$$

Common goals include maximizing the electric field in the target area [111, 113, 114] and minimizing deviations between the electric field distribution and preset values [114, 115, 116]. Some complex objective functions are discussed in Section 4. And the constraints are primarily designed to ensure the safety of human participants (Fig. 1 G). The total injection current and the maximum individual injection current are denoted as  $I_{tot}$  and  $I_{ind}$ , respectively. For  $N$  candidate electrodes, considering the presence of a reference electrode and according to Kirchhoff's current law, Eq. (8) stipulates that the sum of the absolute values of the current intensities of the candidates and the reference electrode should be less than  $2 * I_{tot}$ . The constraints, Eq. (9) and Eq. (10), are designed to prevent discomfort at the individual electrode interface. The values of  $I_{ind}$  and  $I_{tot}$  are typically set to 1 mA and 2 mA, respectively. However, these values can vary depending on the specific experimental design. For example, in some protocols, such as ISP stimulation, the amplitude can reach as high as 7 mA [19].

$$g_1(s) = \sum_n |s_n| + \left| \sum_n s_n \right| \leq 2I_{tot}, \quad (8)$$

$$g_2(s) = |s_n| \leq I_{ind}, \quad (9)$$

$$g_3(s) = \left| \sum_n s_n \right| \leq I_{ind}, \quad (10)$$

Additionally, constraints can be designed to meet various requirements. Ruffini et al. control the number of active electrodes by penalizing unsuitable solutions [43]. Furthermore, Huang et al. limit the power of the electric field outside the target region to manage the trade-offs between maximal intensity and focality [111].

The results of inverse optimization can be directly applied to adjust the stimulation montage in tES, enabling personalized stimulation protocols (Fig. 1 I).

### 3.2 Optimization algorithms for personalized tES

A variety of methods have been proposed for optimizing electrical stimulation strategy. **The exhaustive search algorithm** is a brute-force method which traverses all possible solutions. Its advantage lies in its universality, suitable for tACS and tTIS, even multi-pair tTIS [118], and its ability to obtain the unique, optimal solution of the tES electrode montage and the corresponding injection current [39, 40, 119, 120]. However, given the vast search space, the exhaust search algorithm is extremely slow and computationally intensive. For example, Rampersad et al. reported that they have to evaluate all 146 million candidates in order to identify the optimal tTIS strategy involving 88 electrodes [40].

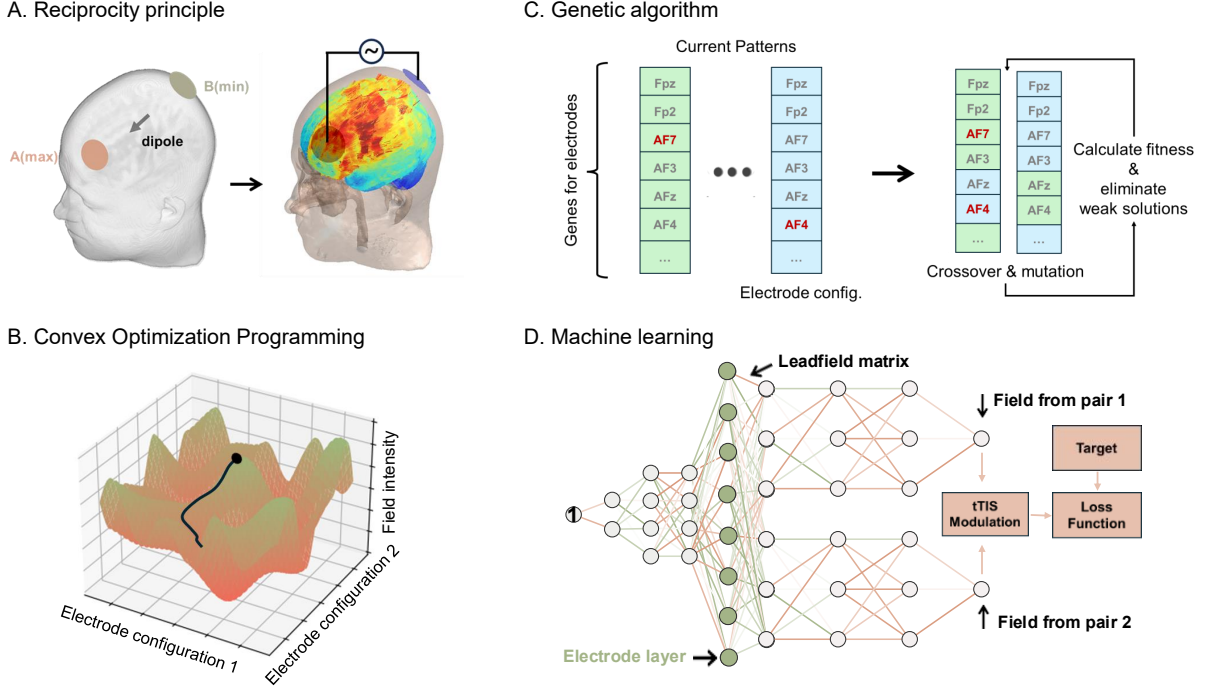


Figure 2: Schematic diagram of the stimulation optimization methods. (A) Reciprocity principle: The Reciprocity Principle posits that the path of electrical current flow from a stimulation electrode placed on the scalp to a designated area within the brain is equivalent to the path of current flow in the reverse direction, from that specific brain area back to the scalp electrode. Consequently, this principle allows for the utilization of a dipole and a simulation model to determine the optimal electrode configuration for targeted stimulation. (B) Convex optimization programming: By iteratively substituting a non-convex problem with solvable convex relaxations or linearized surrogates and refining them, one can leverage convex optimizers to efficiently approach the global optimum of the original formulation. (C) Genetic algorithm: This algorithm encodes electrode configurations into the genes of each solution within a population. Genes represent the activation status of the corresponding channel. The solutions represent a stimulation pattern. During each iteration, the solutions undergo crossover and mutation processes at random, resulting in the generation of offspring. Offspring demonstrating superior performance are retained. Ultimately, we can get the optimal solution at the last iteration. (D) Deep learning: The approach utilizes a neural network in which a constant unit replaces the input. Fully connected layers are used to generate weights within the electrode layer, which features twice as many nodes as the number of electrodes. Utilizing both the electrode layer and the lead field matrix, the distribution of the electrical field and then the loss is calculated. The goal is to optimize the electrode currents that minimize the loss by training the weights of the electrode layer. The panel is adapted from [117].

**The reciprocity principle**, first introduced by Helmholtz in 1853, describes the interchangeability of electrical sources and measurement points in a linear, time-invariant system. It states that the effect of a source at a point in the system (e.g., the brain) can be reciprocated if the source and measurement locations are swapped. Leveraging the reciprocity principle (Fig. 2 A), tES optimization can be approached by first simulating how a source at a target brain location would influence scalp electrodes, and then inverting this relationship to determine optimal electrode placements and activation patterns for effective stimulation of the target[121, 122].

In practical applications, the lead field matrix encodes this forward information. Based on the reciprocity principle, one can simplify the optimization process by selecting the channel exhibiting maximum intensity to derive an optimal stimulation pattern. Fernandez et al.[123] further advanced the understanding of the reciprocity principle by presenting a unified framework encompassing related methods. They theoretically demonstrated that Least Squares (LS), Weighted Least Squares (WLS), and reciprocity-based closed-form solutions are all special cases of the extended directional maximization problem. Moreover, LS/WLS and reciprocity-based solutions represent two extremes of the intensity-focality trade-off inherent in this optimization problem. This insight not only validates the efficacy of the reciprocity principle but also provides a means to characterize the performance bounds of other approaches without requiring extensive computational effort[22, 111].

**Iterative convex and linear optimization solvers** are widely recognized for their efficiency and effectiveness in addressing complex problems [43, 60, 66, 113]. These approaches typically involve maximizing or minimizing carefully formulated objective functions. Variants of Least Squares (LS) optimization and constrained directional maximization are among the most fundamental and widely adopted techniques in this domain. They form the computational backbone of mainstream tES optimization software, such as SimNIBS [71, 82] and ROAST [70], and are crucial for optimizing tTIS [68, 69]. For example, a typical optimization problem in tES aims to maximize the electric field intensity at a predefined orientation while satisfying practical constraints, including a total current budget, upper bounds on field strength within avoidance zones, and per-electrode current limits. In this context, Least Squares methods minimize the second-order error between the achieved and desired electric fields, subject to current constraints [42, 60, 121]. In contrast, constrained directional maximization seeks to directly maximize the target electric field intensity, also under constraints such as current limits [60, 122] or avoidance zone regulations [113, 124].

When both the objective function and the constraints are convex, powerful frameworks like Disciplined Convex Programming (Fig. 2 B) offer effective and scalable solutions [125]. However, more complex or non-convex scenarios necessitate additional algorithmic strategies. For instance, the integration of **branch-and-bound algorithms** enables optimizing systems with a limited number of active electrodes—a non-convex problem [66]. Branch-and-bound methods enhance computational tractability by systematically partitioning the search space and pruning suboptimal regions, ultimately converging to the global optimum. The applicability of convex optimization methods can thus be significantly extended through such hybrid approaches, allowing them to accommodate increasingly complex and realistic constraints.

**Machine learning** has also been utilized to optimize electrode montages, such as genetic algorithms (Fig. 2 C) and neural networks (Fig. 2 D). The genetic algorithm maintains a population of candidate solutions, each solution has a set of properties called chromosomes. The genetic algorithm encodes the active state of each electrical channel into the chromosomes of solutions, subsequently engaging in mutation and crossover processes to recombine these chromosomes. With the evaluation of electrical field by electrode configurations derived from newly generated solutions, algorithm retains those with superior performance while discarding less effective ones. Through iterative execution, the genetic algorithm converges on the optimal solution. This approach exhibits inherent flexibility in managing non-convex formulations and demonstrates remarkable adaptability in tackling objectives and constraints of increased complexity. For example, Ruffini et al. and Lee et al. employed genetic algorithm to optimize multi-focal stimulation [39, 43], and Stoupis et al. used genetic algorithms to achieve focal stimulation over the hippocampus and thalamus using two pairs of tTIS electrodes [87].

Additionally, neural networks have also been employed to address this problem. Bahn et al. applied unsupervised neural networks to optimize tES and achieve multi-target stimulation based on HD-tTIS and HD-tDCS [117]. In this unsupervised neural network, there is no traditional input. Instead, a constant value is propagated through fully connected layers to generate an electrical configuration. Thereafter, a stimulation network calculates the electric field based on this configuration, from which a loss function is derived. Through this mechanism, the neural network optimizes the electrode currents using repeated backpropagation to achieve field aligned with the target.

Achieving **focused stimulation** is a key objective of optimization. However, there is an inherent trade-off between focality and intensity in tES. A stronger intensity within the target often results in increased activation outside the target, particularly for deep brain targets. This trade-off can be managed through additional design strategies. The Weighted Least Squares (Weighted-LS) method can enhance the focus on intensity within the target area by applying a weight matrix [60]. For constrained directional maximization, implementing an extra constraint to limit power outside

the target area offers a means to balance these trade-offs [111]. The basic reciprocity-based method primarily focuses on maximizing stimulation intensity without explicit consideration of focality. Dmochowski et al. [42] addressed this limitation by incorporating L1-constraints, demonstrating that naive maximization strategies can yield suboptimal stimulation patterns. By aligning spatially decorrelated scalp potentials with optimized tES current patterns, they achieved enhanced stimulation efficacy, highlighting the importance of considering spatial focality alongside intensity.

Multi-objective optimization via evolutionary algorithm (**MOVEA**) is another natural solution for addressing the focused stimulation. Wang et al. provide a comprehensive comparison of various modulation methods and objectives based on the Pareto front [22]. This Pareto front consists of optimal solutions that meet various requirements while respecting trade-off relationships between conflicting objectives such as intensity and focality. And MOVEA is versatile and suitable for both tACS and tTIS based on high definition and two-pair systems. Furthermore, most algorithms require the definition of a preferred direction, which may not always be available due to prior knowledge or required data. An alternative approach is to optimize the field strength. MOVEA have proven to be effective in solving it, although this introduces greater complexity due to the need to calculate the norm.

### 3.3 Applications for optimizing tES strategy

Personalized tES montage, in contrast to traditional montage, can achieve more effective targeted neuromodulation [112, 126]. Therefore, inverse optimization has been extensively utilized in research. Mainstream applications respectively rely on computational modeling simulation and optimization algorithm implementation (Table 4). Computational modeling has been used to determine the optimal electrode configuration. Many studies employ multiple stimulation montages in the forward model to identify the effectiveness by analyzing the distribution of the electric field in the brain. Galletta et al. developed a forward model of a patient with left frontal stroke and compared five tDCS montages used in the clinical treatment of aphasia. Mackenbach et al. simulated and demonstrated through computational modeling that increasing the inter-electrode distance in HD-tDCS enhances the electric field strength and stimulation depth [127]. In a subsequent study, they utilized this discovery to customize a personalized montage to investigate the modulating effect of HD-tDCS on upper limb rehabilitation in ischemic stroke patients [128].

Algorithmic optimization is primarily reliant on existing implementations within modeling software. Mainstream software packages such as SimNIBS and ROAST incorporate optimization algorithm pipelines. Many studies utilize optimization results from computational models to design stimulus montages, aiming to minimize individual variability and enhance stimulus efficacy. Hsu et al. investigated the impact of tDCS on sequence learning by employing ROAST to create a forward model of each subject's MRI. They used the targeting pipeline within ROAST to generate a personalized montage, confirming that tDCS facilitation of the motor cortex relies on a sufficiently high electric field strength [129]. Guillen et al. employed the targeting pipeline within ROAST to determine optimal electrode configurations for the MIDA model [130] while investigating the most effective tDCS montage for patients with cranial defects [131].

Furthermore, algorithmic optimization plays a critical role in guiding treatment decisions. Prior research has demonstrated that lesion location significantly influences the local electric field surrounding the stimulation target, resulting in variations in electric field strength [132]. Considering that the efficacy of tES relies on sufficient electric field strength, utilizing optimized results as a treatment paradigm can minimize variability when evaluating treatment outcomes [133]. Machado et al. utilized commercial software HD-Explore to determine electrode positions and current magnitude for HD-tDCS, while examining the effects of tDCS on athletic performance and physiological-psychological responses in athletes [134]. Grover et al. achieved longer-lasting memory enhancement by using optimization results from HD-Targets (version 3.0.1, Soterix Medical) in the treatment of memory function improvement among elderly individuals [25].

Remarkably, algorithmic optimization has garnered positive feedback regarding its therapeutic efficacy. Cruijssen et al. discovered that personalized tDCS montages enhanced intracerebral electric field strength among stroke patients [133]. Rasmussen et al. observed that personalized HD-tDCS notably enhanced delayed memory in Alzheimer's disease (AD) patients compared to conventional electrode montages [10]. Given the superior outcomes demonstrated by personalized tES in both research and treatment, the utilization of optimization algorithms to design stimulation protocols is expected to become increasingly prevalent in future research endeavors. Maximizing the electric field in the brain will minimize the impact of inter-subject differences, resulting in more reliable data for scientific research. This will facilitate the exploration of neuromodulation mechanisms and the expansion of therapeutic applications.

Table 4: Applications for inverse optimization

Reference	Healthy / Diseased Subjects	Report Findings
Kolmos M, et al. (2023). Trials [135]	Diseased Subjects (Ischemic Stroke)	The personalized tDCS group showed a significant improvement in the Fugl-Meyer Assessment of Upper Extremity score.
Khan A, et al. (2023). Brain Stimulation [136]	Healthy Subjects	Targeted and optimized mc-tDCS can outperform standard bipolar stimulation and lead to better control over stimulation outcomes.
Jog MA, et al. (2023). Science Report [137]	Diseased Subjects (Major Depression Disorder)	Serial HD-tDCS leads to neurostructural changes at a predetermined brain target in depression.
Williamson, J. N., et al. (2023). Frontiers in human neuroscience [128]	Diseased Subjects (Ischemic Stroke)	HD-tDCS can improve the function of the lesioned corticospinal tract and reduce the excitability of the contralateral cortico-reticulospinal tract.
Hsu, G., et al. (2023). Brain stimulation [129]	Healthy Subjects	The new electrode montage can achieve stronger motor cortex polarization than alternative montages.
Guillen, A., et al. (2023). Frontiers in human neurosciences [131]	Healthy Subjects	Modeling studies that take advantage of the individual anatomy of skull defects can help guide tDCS practice in patients with skull defects and skull plates.
Caulfield KA, et al. (2022). Neuromodulation [138]	Healthy Subjects	Using reverse-calculation modeling to produce the same high electric fields in the cortex between participants may produce future tDCS treatments more effective for working memory.
Antonenko D, et al. (2022). Alzheimers Dement (N Y) [139]	Healthy Subjects	Improvements in working memory were associated with individually induced electric field strengths.
Grover S, et al. (2022). Nature neuroscience [25]	Diseased Subjects (Memory Impairment)	The aging brain's plasticity can be selectively and sustainably enhanced through focused neuromodulation based on memory-specific cortical circuitry's spatiotemporal parameters.
Soleimani G, et al. (2022). Brain stimulation [140]	Diseased Subjects (Methamphetamine Use Disorder)	Our knowledge about activated brain regions during a specific task and connectivity between active brain regions can be used to resolve ambiguity about electrode locations for network-based modulation of the human brain.

Continued on next page.

van der Cruijsen J, et al. (2022). <i>NeuroImage: Clinical</i> [133]	Diseased Subjects (Chronic Stroke)	Individualized electrode configurations increased the electrical field strength at the anatomical and functional target for stroke subjects.
Klírová M, et al. (2021). <i>Frontiers in Systems Neuroscience</i> [126]	Healthy Subjects	Individualized HD $\theta$ -tACS applied via the mPFC-ACC significantly improves the post-tACS verbal component of conflict-processing.
Rasmussen I D, et al. (2021). <i>Journal of Alzheimer's Disease</i> [10]	Diseased Subjects (AD)	HD-tDCS significantly improved delayed memory in AD.
Suen PJC, et al. (2021). <i>Eur Arch Psychiatry Clin Neurosci</i> [141]	Diseased Subjects (Depression)	EF strength simulations might be associated with further behavioral changes in depressed patients.
da Silva Machado, D. G., et al. (2021). <i>Scientific reports</i> [134]	Healthy Subjects	Neither HD-tDCS nor conventional tDCS changed exercise performance and psychophysiological responses in athletes.
Muffel T, et al. (2019). <i>Front Aging Neurosci</i> [142]	Healthy Subjects	Anodal-tDCS over S1 elicits opposing effects on proprioceptive accuracy as a function of age.

## 4 Enhancing tES Modeling through Multimodal images and Brain-State Feedback

Although computational models hold great promise for personalized tES, a substantial gap remains between current modeling approaches and real-world neuromodulation outcomes. Bridging this gap requires the integration of additional information to dynamically refine models and enhance their ability to regulate brain activity effectively. Model updating primarily involves two aspects. First, anatomical segmentation and anisotropic properties in the head model can be improved using multimodal neuroimaging data (e.g., MRI, DTI), while model parameters such as tissue conductivity can be adjusted based on recorded stimulation responses (e.g., EEG, fMRI). These refinements increase the accuracy of electric field simulations and improve model adaptability to individual-specific anatomical and physiological characteristics. Second, the objective functions of the inverse optimization problem can be revised to reflect brain-state-dependent targets, guided by real-time EEG or fMRI data. Previous studies have shown that the effects of tES are highly contingent on the current functional state of the brain [1, 91]. By leveraging neural signals to infer ongoing brain states, the optimization targets can be dynamically updated, enabling more precise, adaptive, and context-aware neuromodulation.

### 4.1 Refining Forward Models through Segmentation, Conductivity, and Anisotropy Updates

A substantial discrepancy often exists between the electric fields predicted by computational models and those empirically measured (Fig. 3). This mismatch is largely attributable to individual variability in tissue properties and limitations in anatomical segmentation. Improving segmentation fidelity, both in terms of accuracy and anatomical detail, is crucial for enhancing forward modeling precision [79, 143] (Fig. 3 B). For instance, Weise et al. [144] demonstrated that the inclusion of the meninges, often omitted due to computational cost, can significantly alter the peak electric field intensity. Similarly, Wang et al. [145] reported that layered versus single-layer individualized skull models yield markedly different field distributions. These findings underscore the importance of incorporating detailed and individualized tissue definitions into the model. This challenge is further compounded in pediatric or neonatal populations,

where immature tissue development and limitations in imaging resolution complicate segmentation and conductivity estimation [146].

Tissue conductivity is another key issue in modeling electric field distribution [2]. Conductivity values can vary significantly across individuals, tissue temperature, and even stimulation frequency [147]. To accurately set the tissue conductivity values, head model parameters can be calibrated using intracranial recordings, such as intracranial EEG (iEEG), by aligning predicted and measured values in localized brain regions (Fig.3 C). Several techniques have been proposed for estimating and optimizing conductivity, as well as for quantifying the reliability of model predictions [2, 148, 149]. For example, Huang et al. [2] developed an optimization algorithm that adjusts conductivity values to minimize the discrepancy between modeled and observed iEEG potentials. This calibration can enhance field estimation accuracy across the brain.

Most conventional head models simplify conductivity as a scalar value, without considering the anisotropy of conductivity. However, this assumption overlooks the directional complexity of neural tissue. The presence of aligned white matter tracts gives rise to anisotropic conductivity, which significantly influences the spatial distribution of the electric field [150, 151] (Fig.3 D). Suh et al. [152] demonstrated that incorporating anisotropic skull conductivity can reduce off-target electric fields by 12-14%, thus enhancing spatial specificity. A commonly used approach for modeling anisotropy involves constructing conductivity tensors based on diffusion MRI-derived diffusion tensors and fractional anisotropy metrics. These tensors are rescaled according to known tissue conductivity values and integrated into FEM frameworks. This enables more biologically realistic simulations that account for directional dependencies in current propagation.

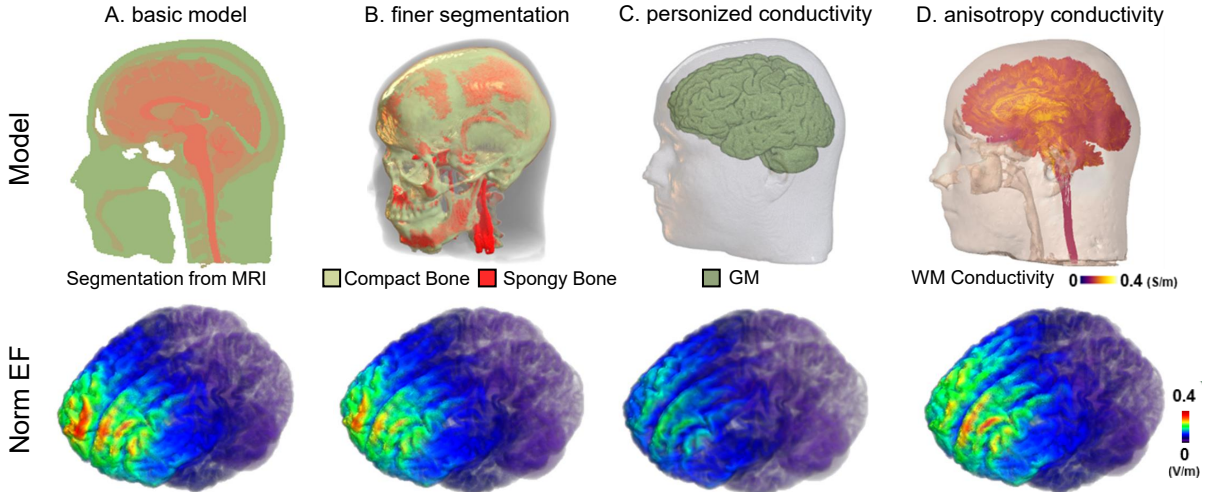


Figure 3: The influence of model updates on the norm of the electrical field. (A) The Standard Model: The upper panel displays a segmentation with five tissue types, each assigned conductivities based on standard values from prior research (WM: 0.126; GM: 0.275; CSF: 1.654; Bone: 0.01; Scalp: 0.465). The lower panel illustrates the distribution of the electric field's magnitude under a 1 mA tDCS from F3 to F4 in the EEG10-10 system. Following visualizations follow the same settings. (B) Bone subdivisions. The bone is segmented into two distinct categories: compact bone with a conductivity of 0.008 and spongy bone with a conductivity of 0.025. (C) Conductivity optimization. The conductivity of Gray Matter is adjusted to its highest reported value in previous research, being 0.6. In practice, conductivity optimization can be combined with sEEG to fine-tune the model's parameters. (D) Anisotropy model. The upper panel depicts the conductivity of White Matter. The conductivity of tissues is configured as anisotropic by direct mapping based on linear rescaling of tensors from diffusion MRI. The upper threshold for conductivity is established at 2 S/m, with a maximum ratio of 10 between the largest and smallest conductivity eigenvalues. The unit of conductivity: S/m. The unit of electrical field: V/m. Abbr: WM, White Matter; GM, Gray Matter; CSF, Cerebrospinal Fluid; EF, electrical field; tDCS, transcranial Direct Current Stimulation.

## 4.2 Incorporating Brain-State Dynamics into Inverse Optimization

Conventional inverse optimization approaches in tES often treat the brain as a passive electrical medium, neglecting its intrinsic nonlinear and state-dependent behavior. However, accumulating evidence suggests that the efficacy of neuromodulation is highly dependent on the brain's dynamic state at the time of stimulation [1, 153]. These brain states—reflected in EEG rhythms, BOLD fluctuations, or patterns of functional connectivity—can critically influence the brain's responsiveness to external stimulation. Accordingly, integrating dynamic brain-state information into the optimization framework represents a key step toward adaptive and truly personalized tES.

One promising direction is to embed brain-state features directly into the objective function of the optimization framework. Rather than minimizing electric field errors in anatomical space alone, state-aware optimization seeks to maximize neuromodulatory efficacy by targeting functionally relevant network states. For example, network controllability theory offers a powerful lens for understanding how exogenous inputs can drive neural systems from one state to another. In this framework, optimal stimulation parameters can be derived by minimizing the energy required to transition the system toward a desirable brain state, given the individual's current functional configuration.

The first step in brain-state-informed optimization is the acquisition of relevant neural signals during tES. EEG is the most widely used modality to assess tES-induced neural changes before and after stimulation [154, 155, 156]. However, accurately capturing brain activity during stimulation remains challenging due to strong electrical artifacts. To address this, alternative modalities such as fMRI and sEEG have been employed for simultaneous recording with tES [156, 157, 158, 159, 160]. These studies have not only demonstrated the efficacy of tES but also revealed significant discrepancies between simulated and empirically observed neural responses [91, 159], highlighting the influence of individual variability and dynamic brain states. One explanation for these discrepancies is the oversimplification of the brain as a linear conductor in computational models. In reality, the brain is a complex, nonlinear, and adaptive system. Recent studies have shown that tES can modulate brain networks rather than isolated regions [71, 161, 162]. For example, Rostami et al. demonstrated that tACS modulates cortical connectivity within the dorsal attention network, as evidenced by changes in phase-locking values [163]. Mulyana et al. further advanced this direction by proposing a closed-loop tES-fMRI framework to optimize individualized stimulation of frontoparietal networks, resulting in enhanced functional connectivity and improved working memory [156]. Krause et al. suggested that individual variability in neuronal phase preference contributes to heterogeneous tES outcomes, which could be better explained using oscillator-based models [1, 164].

To better capture the temporal evolution of brain activity, hidden Markov models (HMMs) have been widely employed. For example, Kasten et al. used HMMs to analyze MEG data collected before and after tACS, revealing that spontaneous brain states and their underlying functional networks vary in susceptibility to stimulation [165]. Extending this approach, Brown et al. applied high-definition alpha-frequency tACS during a continuous performance task while recording fMRI data. Their results demonstrated that stimulation modulated the temporal dynamics of brain states, as identified by HMMs [166]. We can design objective functions based on brain states and obtain corresponding stimulation strategies. Combining the method with control theory, the brain can be modeled as a dynamic system influenced by external input. A simplified representation is given by a discrete-time linear time-invariant system:

$$x(t+1) = Ax(t) + Bu(t), \quad (11)$$

where vector  $x(t) \in \mathbb{R}^N$  denotes the state of the brain network with  $N$  regions at time  $t$ . The matrix  $A \in \mathbb{R}^{N \times N}$  describes the intrinsic connectivity among brain regions, representing the network topology. The matrix  $B$  captures the distribution of external input, and vector  $u(t) \in \mathbb{R}^N$  represents the control signal applied at time  $t$ .

Control strategies can be broadly categorized as either model-driven or data-driven. In model-driven control, matrix  $A$  is usually derived from prior knowledge, such as structural (white matter tracts), functional (statistical dependencies), or effective (causal interactions) connectivity [167, 168, 169]. The leadfield matrix from electrical modeling can serve as matrix  $B$ , quantifying how each electrode influences brain regions. In contrast, data-driven approaches aim to estimate both  $A$  and  $B$  directly from empirical neural recordings. Given time-series data that reflect evolving brain states  $x(t)$ , the goal is to design optimal control inputs  $u(t)$  that drive the system toward desirable cognitive or clinical outcomes.

## 5 Limitations and future directions

We have introduced simulation and optimization techniques for personalized tES. Computational modeling has proven crucial in enhancing tES performance. However, some limitations still hinder tES performance, which should be addressed.

To fully harness the advantages of computational models, their integration with real-world stimulation hardware is essential. However, this integration is complicated by the diversity of stimulation devices and experimental environments. Most models are built on idealized assumptions, such as standardized equipment configurations and accurate parameter settings, which may not reflect real-world conditions. In practice, factors such as head curvature and subject motion during experiments can result in uneven contact pressure between electrodes and the scalp. This may displace electrodes or alter contact quality, ultimately distorting the electric field distribution and reducing stimulation efficacy [170]. Although methods have been developed for real-time electrode localization [171, 172], current tES frameworks generally lack the capability to dynamically account for such variabilities and adapt the model accordingly. Recent studies have begun to explore more adaptive and online modeling strategies to address this limitation [173, 174]. Additionally, variability in electrode properties—such as size, material, and surface texture—can significantly influence stimulation outcomes [175, 176]. Despite its importance, incorporating these properties into optimization algorithms remains challenging, largely due to the absence of well-defined models to quantify their effects. While electrode size has been shown to play a critical role, no universally accepted equations currently exist to capture the influence of other electrode characteristics, such as material composition and geometry.

The analysis of brain signals during tES presents a promising direction, particularly with the emergence of tES devices that support simultaneous neural signal acquisition, thereby enabling the development of closed-loop systems. Among these, EEG is frequently employed alongside tES due to the compatibility of their underlying principles. However, recording EEG during ongoing tES poses significant technical challenges. The stimulation introduces substantial artifacts, often several orders of magnitude larger than the neural signals of interest, and may even saturate EEG amplifiers [3, 177]. In addition to electrical artifacts, physiological noise from sources such as cardiac and respiratory activity further contaminates the EEG recordings [178, 177]. As a result, the signal-to-noise ratio (SNR) is drastically reduced, making direct interpretation of EEG during tES infeasible. To mitigate this issue, denoising techniques have been proposed. Several offline denoising algorithms have been developed for tES-EEG data [179, 180, 181], and more recently, real-time approaches have emerged to facilitate online monitoring of brain activity. For example, Guarneri et al. introduced an adaptive spatial filtering method, known as alternating current regression (AC-REG), specifically designed to attenuate tACS-induced artifacts in real time [182]. Despite these advances, major challenges remain. The most important of these is the lack of ground truth data, which makes it difficult to verify whether the denoised EEG accurately reflects true neural activity or still contains residual artifacts. Moreover, since tES itself modulates brain activity, the denoising process risks removing not only artifacts but also genuine stimulation-induced neural changes. As a result, validating the effectiveness and fidelity of denoised signals remains an open and actively investigated issue [183].

The frequency of the injected current is another critical factor that warrants careful consideration in computational modeling. Contemporary models predominantly emphasize the amplitude of stimulation and the resulting electric field distribution, often overlooking the significant influence of current frequency. In the case of tACS, which typically operates at low frequencies, the quasi-static approximation is commonly employed. This approximation models the electric field at peak current amplitudes, under the assumption that temporal variations in current intensity only scale the magnitude of the electric field without affecting its spatial distribution. Nevertheless, an increasing number of studies have reported that frequency and phase can substantially affect both the distribution and efficacy of stimulation [67, 145]. These effects become especially pronounced at the higher carrier frequencies used in tTIS. For instance, Liu et al. observed a slight but measurable decrease in the field magnitude at temporal interference frequencies exceeding 2 kHz, which may be attributable to frequency-dependent changes in tissue conductivity [184, 185]. Beyond physical field properties, frequency also plays a critical role in shaping neural responses. Variations in stimulation frequency can significantly modulate neuronal excitability and synaptic dynamics, influencing the effectiveness of neuromodulation [186]. Therefore, it is imperative to expand computational models to incorporate frequency-dependent physiological responses. This can be achieved by integrating large-scale concurrent neural recordings and leveraging advanced signal analysis methods. Such data-driven approaches are essential for developing predictive models that elucidate the complex relationship between stimulation frequency and brain function.

Additionally, the orientation of the electrical field is pivotal, as it can dictate the excitatory or inhibitory responses of neurons. Especially for tTIS, which regulated brain by two pairs of electrodes, a given field orientation can significantly enhance the focality of the envelope field. While optimization algorithms have been developed to refine this aspect, there remains a gap in our understanding of how to precisely configure the field's direction for specific targets. In the case of the cerebral cortex, a vertical orientation is commonly employed [60]. However, for other tissues, defining a more precise target necessitates a deeper integration of neuroscience knowledge. Designing the objective function based on advanced neuroimaging could be a viable approach. For instance, fiber orientation obtained through diffusion MRI could be incorporated into the objective function.

## 6 Conclusion

The tES is an effective non-invasive neuromodulation technique for treating neurological diseases and enhancing cognitive performance. Personalized tES implementation is crucial for mitigating variations in electric field distribution resulting from anatomical differences. Forward modeling and inverse optimization are vital stages in the computational modeling of personalized tES, facilitating the refinement of the stimulation strategy. Optimization methods can be utilized to design stimulation strategies that are more focused or multi-targeted. However, how the external tES interacts with the internal brain's activity remains a topic of ongoing discussion. Combining tES with neural signal recording holds promise for analyzing stimulation results and designing more interpretative models.

## Acknowledgement

I would like to express our sincere gratitude to Dr. Zhichao Liang and Dr. Xinken Shen for their invaluable suggestions during the preparation of this manuscript.

## References

- [1] Matthew R. Krause, Pedro G. Vieira, and Christopher C. Pack. Transcranial electrical stimulation: How can a simple conductor orchestrate complex brain activity? *PLOS Biology*, 21, 2023.
- [2] Yu Huang, Anli A Liu, Belen Lafon, Daniel Friedman, Michael Dayan, Xiuyuan Wang, Marom Bikson, Werner K Doyle, Orrin Devinsky, and Lucas C Parra. Measurements and models of electric fields in the in vivo human brain during transcranial electric stimulation. *elife*, 6:e18834, 2017.
- [3] Anli Liu, Mihály Vöröslakos, Greg Kronberg, Simon Henin, Matthew R Krause, Yu Huang, Alexander Opitz, Ashesh Mehta, Christopher C Pack, Bart Krekelberg, et al. Immediate neurophysiological effects of transcranial electrical stimulation. *Nature communications*, 9(1):1–12, 2018.
- [4] Michele Maiella, Elias Paolo Casula, Ilaria Borghi, Martina Assogna, Alessia D'acunto, Valentina Pezzopane, Lucia Mencarelli, Lorenzo Rocchi, Maria Concetta Pellicciari, and Giacomo Koch. Simultaneous transcranial electrical and magnetic stimulation boost gamma oscillations in the dorsolateral prefrontal cortex. *Scientific Reports*, 12, 2022.
- [5] Katharina S Rufener, Mathias S Oechslin, Tino Zaehle, and Martin Meyer. Transcranial alternating current stimulation (tacs) differentially modulates speech perception in young and older adults. *Brain Stimulation*, 9(4):560–565, 2016.
- [6] Vera Moliadze, Leon Sierau, Ekaterina Lychko, Tristan Stenner, Michael Werchowski, Michael Siniatchkin, and Gesa Hartwigsen. After-effects of 10 hz tacs over the prefrontal cortex on phonological word decisions. *Brain stimulation*, 12(6):1464–1474, 2019.
- [7] Amir V Tavakoli and Kyongsik Yun. Transcranial alternating current stimulation (tacs) mechanisms and protocols. *Frontiers in cellular neuroscience*, 11:214, 2017.
- [8] Hyeon Seo and Sung Chan Jun. Relation between the electric field and activation of cortical neurons in transcranial electrical stimulation. *Brain Stimulation*, 12(2):275–289, 2019.
- [9] Dhaval Solanki, Zeynab Rezaee, Anirban Dutta, and Uttama Lahiri. Investigating the feasibility of cerebellar transcranial direct current stimulation to facilitate post-stroke overground gait performance in chronic stroke: a partial least-squares regression approach. *Journal of NeuroEngineering and Rehabilitation*, 18:1–18, 2021.
- [10] Ingrid Daae Rasmussen, Nya Mehnwole Boayue, Matthias Mittner, Martin Bystad, Ole K Grønli, Torgil Riise Vangberg, Gabor Csifcsak, and Per M Aslaksen. High-definition transcranial direct current stimulation improves delayed memory in alzheimer's disease patients: a pilot study using computational modeling to optimize electrode position. *Journal of Alzheimer's Disease*, 83(2):753–769, 2021.
- [11] Sara Simula, Maëva Daoud, Giulio Ruffini, Maria Chiara Biagi, Christian-G Bénar, Pascal Benquet, Fabrice Wendling, and Fabrice Bartolomei. Transcranial current stimulation in epilepsy: A systematic review of the fundamental and clinical aspects. *Frontiers in Neuroscience*, 16:909421, 2022.
- [12] Mengsen Zhang, Rachel B Force, Christopher Walker, Sangtae Ahn, L Fredrik Jarskog, and Flavio Frohlich. Alpha transcranial alternating current stimulation reduces depressive symptoms in people with schizophrenia and auditory hallucinations: a double-blind, randomized pilot clinical trial. *Schizophrenia*, 8(1):114, 2022.

- [13] Matthew R Krause, Pedro G Vieira, Bennett A Csorba, Praveen K Pilly, and Christopher C Pack. Transcranial alternating current stimulation entrains single-neuron activity in the primate brain. *Proceedings of the National Academy of Sciences*, 116(12):5747–5755, 2019.
- [14] Michael A Nitsche and Walter Paulus. Excitability changes induced in the human motor cortex by weak transcranial direct current stimulation. *The Journal of Physiology*, 527, 2000.
- [15] André Russowsky Brunoni, Michael A. Nitsche, Nadia Bolognini, Marom Bikson, Timothy Andrew Wagner, Lotfi B. Merabet, Dylan J. Edwards, Antoni Valero-Cabré, Alexander Rotenberg, Álvaro Pascual-Leone, Roberta Ferrucci, Alberto Priori, Paulo S Boggio, and Felipe Fregni. Clinical research with transcranial direct current stimulation (tdcs): Challenges and future directions. *Brain Stimulation*, 5:175–195, 2012.
- [16] Andrea Antal, Klára Boros, Csaba Poreisz, Leila Chaieb, Daniella Terney, and Walter Paulus. Comparatively weak after-effects of transcranial alternating current stimulation (tacs) on cortical excitability in humans. *Brain Stimulation*, 1:97–105, 2008.
- [17] Marc Bächinger, Valerio Zerbi, Marius Moisa, Rafael Polanía, Quanying Liu, Dante Mantini, Christian C. Ruff, and Nicole Wenderoth. Concurrent tacs-fmri reveals causal influence of power synchronized neural activity on resting state fmri connectivity. *The Journal of Neuroscience*, 37:4766 – 4777, 2017.
- [18] Onno van der Groen and Nicole Wenderoth. Transcranial random noise stimulation of visual cortex: Stochastic resonance enhances central mechanisms of perception. *The Journal of Neuroscience*, 36:5289 – 5298, 2016.
- [19] Mihály Vöröslakos, Yuichi Takeuchi, Kitti Brinyiczki, Tamás Zombori, Azahara Oliva, Antonio Fernández-Ruiz, Gábor Kozák, Zsigmond Tamás Kincses, Béla Iványi, György Buzsáki, et al. Direct effects of transcranial electric stimulation on brain circuits in rats and humans. *Nature communications*, 9(1):483, 2018.
- [20] Nir Grossman, David Bono, Nina Dedic, Suhasa B Kodandaramaiah, Andrii Rudenko, Ho-Jun Suk, Antonino M Cassara, Esra Neufeld, Niels Kuster, Li-Huei Tsai, et al. Noninvasive deep brain stimulation via temporally interfering electric fields. *cell*, 169(6):1029–1041, 2017.
- [21] Ines R Violante, Ketevan Alania, Antonino M Cassarà, Esra Neufeld, Emma Acerbo, Romain Carron, Adam Williamson, Danielle L Kurtin, Edward Rhodes, Adam Hampshire, et al. Non-invasive temporal interference electrical stimulation of the human hippocampus. *bioRxiv*, pages 2022–09, 2022.
- [22] Mo Wang, Kexin Lou, Zeming Liu, Pengfei Wei, and Quanying Liu. Multi-objective optimization via evolutionary algorithm (movea) for high-definition transcranial electrical stimulation of the human brain. *NeuroImage*, 280, 2022.
- [23] Ines R Violante, Ketevan Alania, Antonino M Cassarà, Esra Neufeld, Emma Acerbo, Romain Carron, Adam Williamson, Danielle L Kurtin, Edward Rhodes, Adam Hampshire, et al. Non-invasive temporal interference electrical stimulation of the human hippocampus. *Nature neuroscience*, 26(11):1994–2004, 2023.
- [24] Weiwei Ma, Feixue Wang, Yangyang Yi, Yu Huang, Xinying Li, Ya’ou Liu, and Yiheng Tu. Mapping the electric field of high-definition transcranial electrical stimulation across the lifespan. *Science Bulletin*, 69(24):3876–3888, 2024.
- [25] Shrey Grover, Wen Wen, Vighnesh Viswanathan, Christopher T Gill, and Robert MG Reinhart. Long-lasting, dissociable improvements in working memory and long-term memory in older adults with repetitive neuromodulation. *Nature neuroscience*, 25(9):1237–1246, 2022.
- [26] Siwei Bai, Colleen Loo, and Socrates Dokos. A review of computational models of transcranial electrical stimulation. *Critical Reviews™ in Biomedical Engineering*, 41(1), 2013.
- [27] André Russowsky Brunoni, Pedro Shiozawa, Dennis Q. Truong, Daniel C. Javitt, Helio Elkis, Felipe Fregni, and Marom Bikson. Understanding tdcS effects in schizophrenia: a systematic review of clinical data and an integrated computation modeling analysis. *Expert Review of Medical Devices*, 11:383 – 394, 2014.
- [28] Marom Bikson. History and recent advancements and changes in computational modeling methods for transcranial electrical stimulation. *Brain Stimulation*, 14, 2021.
- [29] Fatemeh Yavari, Asif Jamil, Mohsen Mosayebi Samani, Liliane Pinto Vidor, and Michael A Nitsche. Basic and functional effects of transcranial electrical stimulation (tes)—an introduction. *Neuroscience & Biobehavioral Reviews*, 85:81–92, 2018.
- [30] Shuzhi Chang. The application of transcranial electrical stimulation in sports psychology. *Computational and Mathematical Methods in Medicine*, 2022, 2022.
- [31] JSA Lee, S Bestmann, and C Evans. A future of current flow modelling for transcranial electrical stimulation? *Current Behavioral Neuroscience Reports*, 8(4):150–159, 2021.

[32] Alan C Evans, D Louis Collins, SR Mills, Edward D Brown, Ryan L Kelly, and Terry M Peters. 3d statistical neuroanatomical models from 305 mri volumes. In *1993 IEEE conference record nuclear science symposium and medical imaging conference*, pages 1813–1817. IEEE, 1993.

[33] Vladimir Fonov, Alan C Evans, Kelly Botteron, C Robert Almlí, Robert C McKinstry, D Louis Collins, Brain Development Cooperative Group, et al. Unbiased average age-appropriate atlases for pediatric studies. *Neuroimage*, 54(1):313–327, 2011.

[34] John C Mazziotta, Arthur W Toga, Alan Evans, Peter Fox, Jack Lancaster, et al. A probabilistic atlas of the human brain: theory and rationale for its development. *Neuroimage*, 2(2):89–101, 1995.

[35] Florian H Kasten, Katharina Duecker, Marike C Maack, Arnd Meiser, and Christoph S Herrmann. Integrating electric field modeling and neuroimaging to explain inter-individual variability of tacs effects. *Nature communications*, 10(1):5427, 2019.

[36] Jill von Conta, Florian H Kasten, Branislava Ćurčić-Blake, André Aleman, Axel Thielscher, and Christoph S Herrmann. Interindividual variability of electric fields during transcranial temporal interference stimulation (ttis). *Scientific Reports*, 11(1):1–12, 2021.

[37] Daria Antonenko, Ulrike Grittner, Guilherme Saturnino, Till Nierhaus, Axel Thielscher, and Agnes Flöel. Inter-individual and age-dependent variability in simulated electric fields induced by conventional transcranial electrical stimulation. *Neuroimage*, 224:117413, 2021.

[38] Alexander Hunold, Jens Haueisen, Frauke Nees, and Vera Moliadze. Review of individualized current flow modeling studies for transcranial electrical stimulation. *Journal of Neuroscience Research*, 101(4):405–423, 2023.

[39] Sangjun Lee, Chany Lee, Jimin Park, and Chang-Hwan Im. Individually customized transcranial temporal interference stimulation for focused modulation of deep brain structures: a simulation study with different head models. *Scientific reports*, 10(1):1–11, 2020.

[40] Sumientra Rampersad, Biel Roig-Solvas, Mathew Yarossi, Praveen P Kulkarni, Emiliano Santarecchi, Alan D Dorval, and Dana H Brooks. Prospects for transcranial temporal interference stimulation in humans: a computational study. *NeuroImage*, 202:116124, 2019.

[41] Gehan Abouelseoud, Yasmine Abouelseoud, Amin A. Shoukry, Nour Ismail, and Jaidaa Mekky. A mixed integer linear programming approach to electrical stimulation optimization problems. *IEEE Transactions on Neural Systems and Rehabilitation Engineering*, 26:527–537, 2018.

[42] Jacek P Dmochowski, Laurent Koessler, Anthony M Norcia, Marom Bikson, and Lucas C Parra. Optimal use of eeg recordings to target active brain areas with transcranial electrical stimulation. *Neuroimage*, 157:69–80, 2017.

[43] Giulio Ruffini, Michael D Fox, Oscar Ripolles, Pedro Cavaleiro Miranda, and Alvaro Pascual-Leone. Optimization of multifocal transcranial current stimulation for weighted cortical pattern targeting from realistic modeling of electric fields. *Neuroimage*, 89:216–225, 2014.

[44] Pedro Cavaleiro Miranda, Mikhail Lomarev, and Mark Hallett. Modeling the current distribution during transcranial direct current stimulation. *Clinical neurophysiology*, 117(7):1623–1629, 2006.

[45] Yu Huang, Lucas C Parra, and Stefan Haufe. The new york head—a precise standardized volume conductor model for eeg source localization and tes targeting. *NeuroImage*, 140:150–162, 2016.

[46] Shiva Asadzadeh, Tohid Yousefi Rezaii, Soosan Beheshti, Azra Delpak, and Saeed Meshgini. A systematic review of eeg source localization techniques and their applications on diagnosis of brain abnormalities. *Journal of Neuroscience Methods*, 339:108740, 2020.

[47] Mohammad Ali Salehinejad, Vahid Nejati, Mohsen Mosayebi-Samani, Ali Mohammadi, Miles Wischniewski, Min-Fang Kuo, Alessio Avenanti, Carmelo M Vicario, and Michael A Nitsche. Transcranial direct current stimulation in adhd: a systematic review of efficacy, safety, and protocol-induced electrical field modeling results. *Neuroscience bulletin*, 36:1191–1212, 2020.

[48] Ioannis Zorzos, Ioannis Kakkos, Errikos M Ventouras, and George K Matsopoulos. Advances in electrical source imaging: A review of the current approaches, applications and challenges. *Signals*, 2(3):378–391, 2021.

[49] M-P Dubuisson and Anil K Jain. A modified hausdorff distance for object matching. In *Proceedings of 12th international conference on pattern recognition*, volume 1, pages 566–568. IEEE, 1994.

[50] Tawfik B Khalil and Robert P Hubbard. Parametric study of head response by finite element modeling. *Journal of Biomechanics*, 10(2):119–132, 1977.

[51] Tim A Wagner, Markus Zahn, Alan J Grodzinsky, and Alvaro Pascual-Leone. Three-dimensional head model simulation of transcranial magnetic stimulation. *IEEE Transactions on Biomedical Engineering*, 51(9):1586–1598, 2004.

[52] Tim Wagner, Felipe Fregni, Shirley Fecteau, Alan Grodzinsky, Markus Zahn, and Alvaro Pascual-Leone. Transcranial direct current stimulation: a computer-based human model study. *Neuroimage*, 35(3):1113–1124, 2007.

[53] FS Salinas, JL Lancaster, and PT Fox. 3d modeling of the total electric field induced by transcranial magnetic stimulation using the boundary element method. *Physics in Medicine & Biology*, 54(12):3631, 2009.

[54] Manfred Fuchs, Jörn Kastner, Michael Wagner, Susan Hawes, and John S Ebersole. A standardized boundary element method volume conductor model. *Clinical neurophysiology*, 113(5):702–712, 2002.

[55] Nasireh Dayarian and Ali Khadem. Evaluating the performance of the hybrid boundary element-finite element (be-fe) method to solve electroencephalography (eeg) forward problem based on the mesh quality: A simulation study. *Frontiers in Biomedical Technologies*, 2023.

[56] Anna Šušnjara, Ožbej Verhnik, Dragan Poljak, Mario Cvetković, and Jure Ravnik. Stochastic-deterministic boundary element modelling of transcranial electric stimulation using a three layer head model. *Engineering Analysis with Boundary Elements*, 123:70–83, 2021.

[57] Anna Susnjara, Jure Ravnik, Ozbej Verhnik, Dragan Poljak, and Mario Cvetković. Stochastic-deterministic boundary integral method for transcranial electric stimulation: a cylindrical head representation. In *2019 International Conference on Software, Telecommunications and Computer Networks (SoftCOM)*, pages 1–7. IEEE, 2019.

[58] Anna Šušnjara, Ožbej Verhnik, Dragan Poljak, Mario Cvetković, and Jure Ravnik. Uncertainty quantification and sensitivity analysis of transcranial electric stimulation for 9-subdomain human head model. *Engineering Analysis with Boundary Elements*, 135:1–11, 2022.

[59] Sergei Turovets, Vasily Volkov, Aleksej Zherdetsky, Alena Prakonina, Allen D Malony, et al. A 3d finite-difference bicg iterative solver with the fourier-jacobi preconditioner for the anisotropic eit/eeg forward problem. *Computational and mathematical methods in medicine*, 2014, 2014.

[60] Jacek P Dmochowski, Abhishek Datta, Marom Bikson, Yuzhuo Su, and Lucas C Parra. Optimized multi-electrode stimulation increases focality and intensity at target. *Journal of neural engineering*, 8(4):046011, 2011.

[61] Patrick Dular, Christophe Geuzaine, François Henrotte, and Willy Legros. A general environment for the treatment of discrete problems and its application to the finite element method. *IEEE Transactions on Magnetics*, 34(5):3395–3398, 1998.

[62] Abhishek Datta, Varun Bansal, Julian Diaz, Jinal Patel, Davide Reato, and Marom Bikson. Gyri-precise head model of transcranial direct current stimulation: improved spatial focality using a ring electrode versus conventional rectangular pad. *Brain stimulation*, 2(4):201–207, 2009.

[63] Sumientra M Rampersad, Arno M Janssen, Felix Lucka, Ümit Aydin, Benjamin Lanfer, Seok Lew, Carsten H Wolters, Dick F Stegeman, and Thom F Oostendorp. Simulating transcranial direct current stimulation with a detailed anisotropic human head model. *IEEE Transactions on Neural Systems and Rehabilitation Engineering*, 22(3):441–452, 2014.

[64] Hamzah Magsood and RL Hadimani. Development of anatomically accurate brain phantom for experimental validation of stimulation strengths during tms. *Materials Science and Engineering: C*, 120:111705, 2021.

[65] Luis J Gomez, Moritz Dannhauer, Lari M Koponen, and Angel V Peterchev. Conditions for numerically accurate tms electric field simulation. *Brain stimulation*, 13(1):157–166, 2020.

[66] Guilherme Bicalho Saturnino, Hartwig Roman Siebner, Axel Thielscher, and Kristoffer Hougaard Madsen. Accessibility of cortical regions to focal tes: Dependence on spatial position, safety, and practical constraints. *NeuroImage*, 203:116183, 2019.

[67] Guilherme Bicalho Saturnino, Kristoffer Hougaard Madsen, Hartwig Roman Siebner, and Axel Thielscher. How to target inter-regional phase synchronization with dual-site transcranial alternating current stimulation. *Neuroimage*, 163:68–80, 2017.

[68] Yu Huang, Abhishek Datta, and Lucas C Parra. Optimization of interferential stimulation of the human brain with electrode arrays. *Journal of neural engineering*, 17(3):036023, 2020.

[69] Yu Huang and Lucas C Parra. Can transcranial electric stimulation with multiple electrodes reach deep targets? *Brain stimulation*, 12(1):30–40, 2019.

[70] Yu Huang, Abhishek Datta, Marom Bikson, and Lucas C Parra. Realistic volumetric-approach to simulate transcranial electric stimulation—roast—a fully automated open-source pipeline. *Journal of neural engineering*, 16(5):056006, 2019.

[71] Guilherme B Saturnino, Kristoffer H Madsen, and Axel Thielscher. Optimizing the electric field strength in multiple targets for multichannel transcranial electric stimulation. *Journal of neural engineering*, 18(1):014001, 2021.

[72] Moritz Dannhauer, Dana Brooks, Don Tucker, and Rob MacLeod. A pipeline for the simulation of transcranial direct current stimulation for realistic human head models using scirun/biomesh3d. In *2012 Annual International Conference of the IEEE Engineering in Medicine and Biology Society*, pages 5486–5489. IEEE, 2012.

[73] Young-Jin Jung, Jung-Hoon Kim, and Chang-Hwan Im. Comets: A matlab toolbox for simulating local electric fields generated by transcranial direct current stimulation (tdcs). *Biomedical engineering letters*, 3:39–46, 2013.

[74] S Wagner, SM Rampersad, Ü Aydin, J Vorwerk, TF Oostendorp, T Neuling, CS Herrmann, DF Stegeman, and CH Wolters. Investigation of tdcS volume conduction effects in a highly realistic head model. *Journal of neural engineering*, 11(1):016002, 2013.

[75] Bruce Fischl. Freesurfer. *Neuroimage*, 62(2):774–781, 2012.

[76] Mark Jenkinson, Christian F. Beckmann, Timothy E.J. Behrens, Mark W. Woolrich, and Stephen M. Smith. Fsl. *NeuroImage*, 62(2):782–790, 2012. 20 YEARS OF fMRI.

[77] Mirko Windhoff, Alexander Opitz, and Axel Thielscher. Electric field calculations in brain stimulation based on finite elements: an optimized processing pipeline for the generation and usage of accurate individual head models. Technical report, Wiley Online Library, 2013.

[78] Jesper D Nielsen, Kristoffer H Madsen, Oula Puonti, Hartwig R Siebner, Christian Bauer, Camilla Gøbel Madsen, Guilherme B Saturnino, and Axel Thielscher. Automatic skull segmentation from mr images for realistic volume conductor models of the head: Assessment of the state-of-the-art. *Neuroimage*, 174:587–598, 2018.

[79] Oula Puonti, Koen Van Leemput, Guilherme B Saturnino, Hartwig R Siebner, Kristoffer H Madsen, and Axel Thielscher. Accurate and robust whole-head segmentation from magnetic resonance images for individualized head modeling. *Neuroimage*, 219:117044, 2020.

[80] Sybren Van Hoornweder, Raf L. J. Meesen, and Kevin A. Caulfield. On the importance of using both t1-weighted and t2-weighted structural magnetic resonance imaging scans to model electric fields induced by non-invasive brain stimulation in simnibs. *Brain Stimulation*, 15:641–644, 2022.

[81] Anh Phong Tran, Shijie Yan, and Qianqian Fang. Improving model-based fnirs analysis using mesh-based anatomical and light-transport models. *bioRxiv*, 2020.

[82] Guilherme B Saturnino, Oula Puonti, Jesper D Nielsen, Daria Antonenko, Kristoffer H Madsen, and Axel Thielscher. Simnibs 2.1: a comprehensive pipeline for individualized electric field modelling for transcranial brain stimulation. *Brain and human body modeling*, pages 3–25, 2019.

[83] François Tadel, Sylvain Baillet, John C. Mosher, Dimitrios Pantazis, and Richard M. Leahy. Brainstorm: A user-friendly application for meg/eeg analysis. *Computational Intelligence and Neuroscience*, 2011, 2011.

[84] Takfarinas Medani, Juan Garcia-Prieto, François Tadel, Marios Antonakakis, Tim Erdbrügger, Malte B. Höller-shinken, Wayne Mead, Sophie Schrader, Anand A. Joshi, Christian Engwer, Carsten H. Wolters, John C. Mosher, and Richard M. Leahy. Brainstorm-duneuro: An integrated and user-friendly finite element method for modeling electromagnetic brain activity. *NeuroImage*, 267:119851 – 119851, 2023.

[85] Anke Ninija Karabanov, Guilherme Bicalho Saturnino, Axel Thielscher, and Hartwig Roman Siebner. Can transcranial electrical stimulation localize brain function? *Frontiers in psychology*, 10:213, 2019.

[86] COMSOL Multiphysics. Introduction to comsol multiphysics®. *COMSOL Multiphysics, Burlington, MA, accessed Feb, 9(2018):32*, 1998.

[87] Dimitrios Stoupis and Theodoros Samaras. Non-invasive stimulation with temporal interference: Optimization of the electric field deep in the brain with the use of a genetic algorithm. *Journal of Neural Engineering*, 19(5):056018, 2022.

[88] Bernhard A Sabel, Anton Kresinsky, Lizbeth Cárdenas-Morales, Jens Haueisen, Alexander Hunold, Moritz Dannhauer, and Andrea Antal. Evaluating current density modeling of non-invasive eye and brain electrical stimulation using phosphene thresholds. *IEEE Transactions on Neural Systems and Rehabilitation Engineering*, 29:2133–2141, 2021.

[89] Minmin Wang, Tao Feng, Hongjie Jiang, Junming Zhu, Wuwei Feng, Pratik Y Chhatbar, Jianmin Zhang, and Shaomin Zhang. In vivo measurements of electric fields during cranial electrical stimulation in the human brain. *Frontiers in Human Neuroscience*, 16:829745, 2022.

[90] Nicholas WG Murray, Petra L Graham, Paul F Sowman, and Greg Savage. Theta tacs impairs episodic memory more than tdc. *Scientific Reports*, 13(1):716, 2023.

[91] Huichun Luo, Xiaolai Ye, Hui-Ting Cai, Mo Wang, Yue Wang, Qiangqiang Liu, Ying Xu, Ziyu Mao, Yanqing Cai, Jing Hong, et al. Frequency-specific and state-dependent neural responses to brain stimulation. *Molecular Psychiatry*, pages 1–11, 2025.

[92] Clément Dondé, Laure Fivel, Frédéric Haesebaert, Emmanuel Poulet, Marine Mondino, and Jérôme Brunelin. Mechanistic account of the left auditory cortex for tone-matching in schizophrenia: A pilot transcranial random noise stimulation (trns) sham-controlled study. *Asian Journal of Psychiatry*, 92:103879, 2024.

[93] Aidan Lewis, Constantino Toufexis, Chloe Goldsmith, Rebecca Robinson, Grace Howie, Ben Rattray, and Andrew Flood. The effects of transcranial direct current stimulation and exercise on salivary s100b protein indicated blood-brain barrier permeability: A pilot study. *Neuromodulation: Technology at the Neural Interface*, 2023.

[94] Weiming Sun, Xiangli Dong, Guohua Yu, Lang Shuai, Yefeng Yuan, and Chaolin Ma. Transcranial direct current stimulation in patients after decompressive craniectomy: A finite element model to investigate factors affecting the cortical electric field. *Journal of International Medical Research*, 49(2):0300060520942112, 2021.

[95] Carolin Breitling, Tino Zaehle, Moritz Dannhauer, Björn Bonath, Jana Tegelbecker, Hans-Henning Flechtnner, and Kerstin Krauel. Improving interference control in adhd patients with transcranial direct current stimulation (tdcs). *Frontiers in cellular neuroscience*, 10:72, 2016.

[96] Ilkka Laakso and Akimasa Hirata. Computational analysis shows why transcranial alternating current stimulation induces retinal phosphenes. *Journal of neural engineering*, 10(4):046009, 2013.

[97] Hiroki Hamajima, Jose Gomez-Tames, Shintaro Uehara, Yohei Otaka, Satoshi Tanaka, and Akimasa Hirata. Computation of group-level electric field in lower limb motor area for different tdc montages. *Clinical Neurophysiology*, 150:69–78, 2023.

[98] Hanna Lu, Jing Li, Li Zhang, Sandra Sau Man Chan, Linda Chiu Wa Lam, and Open Access Series of Imaging Studies. Dynamic changes of region-specific cortical features and scalp-to-cortex distance: implications for transcranial current stimulation modeling. *Journal of NeuroEngineering and Rehabilitation*, 18:1–12, 2021.

[99] Shinya Uenishi, Atsushi Tamaki, Shinichi Yamada, Kasumi Yasuda, Natsuko Ikeda, Yuki Mizutani-Tiebel, Daniel Keeser, Frank Padberg, Tomikimi Tsuji, Sohei Kimoto, et al. Computational modeling of electric fields for prefrontal tdc across patients with schizophrenia and mood disorders. *Psychiatry Research: Neuroimaging*, 326:111547, 2022.

[100] Mi-Jeong Yoon, Hye Jung Park, Yeun Jie Yoo, Hyun Mi Oh, Sun Im, Tae-Woo Kim, and Seong Hoon Lim. Electric field simulation and appropriate electrode positioning for optimized transcranial direct current stimulation of stroke patients: an in silico model. *Scientific Reports*, 14(1):2850, 2024.

[101] Fatemeh Sadeghikhassanabadi, Jonas Misselhorn, Christian Gerloff, and Simone Zittel. Optimizing the montage for cerebellar transcranial alternating current stimulation (tacs): a combined computational and experimental study. *Journal of Neural Engineering*, 19(2):026060, 2022.

[102] Tulika Nandi, Oula Puonti, William T. Clarke, Caroline Nettekoven, Helen C. Barron, James Kolasinski, Taylor Hanayik, Emily L. Hinson, Adam Berrington, Velicia Bachtiar, Ainslie Johnstone, Anderson M. Winkler, Axel Thielscher, Heidi Johansen-Berg, and Charlotte Jane Stagg. tdc induced gaba change is associated with the simulated electric field in m1, an effect mediated by grey matter volume in the mrs voxel. *Brain stimulation*, 15:1153 – 1162, 2022.

[103] Sybren Van Hoornweder, Kevin A Caulfield, Michael Nitsche, Axel Thielscher, and Raf L J Meesen. Addressing transcranial electrical stimulation variability through prospective individualized dosing of electric field strength in 300 participants across two samples: the 2-spod approach. *Journal of Neural Engineering*, 19, 2022.

[104] Florian H. Kasten, Katharina Duecker, Marike Christiane Maack, Arnd Meiser, and Christoph Siegfried Herrmann. Integrating electric field modeling and neuroimaging to explain inter-individual variability of tacs effects. *Nature Communications*, 10, 2019.

[105] Nicole R. Nissim, Andrew M. O’Shea, Aprinda Indahlastari, Jessica N. Kraft, Olivia von Mering, Serkan Aksu, Eric C. Porges, Ronald A. Cohen, and Adam J. Woods. Effects of transcranial direct current stimulation paired with cognitive training on functional connectivity of the working memory network in older adults. *Frontiers in Aging Neuroscience*, 11, 2019.

[106] Guilherme Bicalho Saturnino, Kristoffer Hougaard Madsen, Hartwig Roman Siebner, and Axel Thielscher. How to target inter-regional phase synchronization with dual-site transcranial alternating current stimulation. *NeuroImage*, 163:68–80, 2017.

[107] I. Alekseichuk, Zsolt Turi, Gabriel Amador de Lara, Andrea Antal, and Walter Paulus. Spatial working memory in humans depends on theta and high gamma synchronization in the prefrontal cortex. *Current Biology*, 26:1513–1521, 2016.

[108] Andreas Christ, Wolfgang Kainz, Eckhart G Hahn, Katharina Honegger, Marcel Zefferer, Esra Neufeld, Wolfgang Rascher, Rolf Janka, Werner Bautz, Ji Chen, et al. The virtual family—development of surface-based anatomical models of two adults and two children for dosimetric simulations. *Physics in Medicine & Biology*, 55(2):N23, 2009.

[109] Ilkka Laakso, Satoshi Tanaka, Soichiro Koyama, Valerio De Santis, and Akimasa Hirata. Inter-subject variability in electric fields of motor cortical tdes. *Brain stimulation*, 8(5):906–913, 2015.

[110] Carys Evans, Clarissa Bachmann, Jenny SA Lee, Evridiki Gregoriou, Nick Ward, and Sven Bestmann. Dose-controlled tdcS reduces electric field intensity variability at a cortical target site. *Brain stimulation*, 13(1):125–136, 2020.

[111] Yu Huang, Chris Thomas, Abhishek Datta, and Lucas C Parra. Optimized tdcS for targeting multiple brain regions: an integrated implementation. In *2018 40th Annual International Conference of the IEEE Engineering in Medicine and Biology Society (EMBC)*, pages 3545–3548. IEEE, 2018.

[112] Kevin A Caulfield and Mark S George. Optimizing transcranial direct current stimulation (tdcs) electrode position, size, and distance doubles the on-target cortical electric field: Evidence from 3000 human connectome project models. *bioRxiv*, pages 2021–11, 2021.

[113] Seyhmust Guler, Moritz Dannhauer, Burak Erem, Rob Macleod, Don Tucker, Sergei Turovets, Phan Luu, Deniz Erdogmus, and Dana H Brooks. Optimization of focality and direction in dense electrode array transcranial direct current stimulation (tdcs). *Journal of neural engineering*, 13(3):036020, 2016.

[114] Jacek P. Dmochowski, Abhishek Datta, Marom Bikson, Yuzhuo Su, and Lucas C. Parra. Optimized multi-electrode stimulation increases focality and intensity at target. *Journal of Neural Engineering*, 8:046011, 2011.

[115] Jacek P. Dmochowski, Laurent Koessler, Anthony Norcia, Marom Bikson, and Lucas C. Parra. Optimal use of eeg recordings to target active brain areas with transcranial electrical stimulation. *NeuroImage*, 157:69 – 80, 2016.

[116] Adnan Salman, Allen D. Malony, Sergei Turovets, Vasily Volkov, David Ozog, and Don M. Tucker. Concurrency in electrical neuroinformatics: parallel computation for studying the volume conduction of brain electrical fields in human head tissues. *Concurrency and Computation: Practice and Experience*, 28:2213 – 2236, 2016.

[117] Sangkyu Bahn, Chany Lee, and Bo-Yeong Kang. A computational study on the optimization of transcranial temporal interfering stimulation with high-definition electrodes using unsupervised neural networks. Technical report, Wiley Online Library, 2023.

[118] Sangjun Lee, Jimin Park, Chany Lee, Chang-Hwan Im, et al. Multipair transcranial temporal interference stimulation for improved focalized stimulation of deep brain regions: A simulation study. *Computers in Biology and Medicine*, 143:105337, 2022.

[119] Ivan Alekseichuk, Arnaud Y Falchier, Gary Linn, Ting Xu, Michael P Milham, Charles E Schroeder, and Alexander Opitz. Electric field dynamics in the brain during multi-electrode transcranial electric stimulation. *Nature communications*, 10(1):1–10, 2019.

[120] Yu Huang and Abhishek Datta. Comparison of optimized interferential stimulation using two pairs of electrodes and two arrays of electrodes. In *2021 43rd Annual International Conference of the IEEE Engineering in Medicine & Biology Society (EMBC)*, pages 4180–4183. IEEE, 2021.

[121] Mariano Fernandez-Corazza, Sergei Turovets, Phan Luu, Erik Anderson, and Don Tucker. Transcranial electrical neuromodulation based on the reciprocity principle. *Frontiers in psychiatry*, 7:87, 2016.

[122] Andrea Cancelli, Carlo Cottone, Franca Tecchio, Dennis Q Truong, Jacek Dmochowski, and Marom Bikson. A simple method for eeg guided transcranial electrical stimulation without models. *Journal of neural engineering*, 13(3):036022, 2016.

[123] Mariano Fernandez-Corazza, Sergei Turovets, and Carlos Horacio Muravchik. Unification of optimal targeting methods in transcranial electrical stimulation. *Neuroimage*, 209:116403, 2020.

[124] Seyhmus Guler, Moritz Dannhauer, Burak Erem, Rob Macleod, Don Tucker, Sergei Turovets, Phan Luu, Waleed Meleis, and Dana H Brooks. Optimizing stimulus patterns for dense array tdcS with fewer sources than electrodes using a branch and bound algorithm. In *2016 IEEE 13th International Symposium on Biomedical Imaging (ISBI)*, pages 229–232. IEEE, 2016.

[125] Michael Grant and Stephen Boyd. Cvx: Matlab software for disciplined convex programming, version 2.1, 2014.

[126] Monika Klírová, Veronika Voráčková, Jiří Horáček, Pavel Mohr, Juraj Jonáš, Daniela Urbaczka Dudysová, Lenka Kostýlková, Dan Fayette, Lucie Krejčová, Silvie Baumann, et al. Modulating inhibitory control processes using individualized high definition theta transcranial alternating current stimulation (hd  $\theta$ -tacs) of the anterior cingulate and medial prefrontal cortex. *Frontiers in Systems Neuroscience*, 15:611507, 2021.

[127] Caroline Mackenbach, Runfeng Tian, and Yuan Yang. Effects of electrode configurations and injected current intensity on the electrical field of transcranial direct current stimulation: A simulation study. In *2020 42nd Annual International Conference of the IEEE Engineering in Medicine & Biology Society (EMBC)*, pages 3517–3520. IEEE, 2020.

[128] Jordan N Williamson, Shirley Ann James, Dorothy He, Sheng Li, Evgeny V Sidorov, and Yuan Yang. High-definition transcranial direct current stimulation for upper extremity rehabilitation in moderate-to-severe ischaemic stroke-a pilot study. *Frontiers in Human Neuroscience*, 17:1286238, 2023.

[129] Gavin Hsu, A Duke Shereen, Leonardo G Cohen, and Lucas C Parra. Robust enhancement of motor sequence learning with 4 mA transcranial electric stimulation. *Brain stimulation*, 16(1):56–67, 2023.

[130] Maria Ida Iacono, Esra Neufeld, Esther Akinnagbe, Kelsey Bower, Johanna Wolf, Ioannis Vogiatzis Oikonomidis, Deepika Sharma, Bryn Lloyd, Bertram J Wilm, Michael Wyss, et al. Mida: a multimodal imaging-based detailed anatomical model of the human head and neck. *PloS one*, 10(4):e0124126, 2015.

[131] Alexander Guillen, Dennis Q Truong, Abhishek Datta, and Yu Huang. Optimized high-definition tdcS in patients with skull defects and skull plates. *Frontiers in Human Neuroscience*, 17, 2023.

[132] Jacek P Dmochowski, Abhishek Datta, Yu Huang, Jessica D Richardson, Marom Bikson, Julius Fridriksson, and Lucas C Parra. Targeted transcranial direct current stimulation for rehabilitation after stroke. *Neuroimage*, 75:12–19, 2013.

[133] Joris van der Cruisen, Renée F Dooren, Alfred C Schouten, Thom F Oostendorp, Maarten A Frens, Gerard M Ribbers, Frans CT van der Helm, Gert Kwakkel, Ruud W Selles, et al. Addressing the inconsistent electric fields of tdcS by using patient-tailored configurations in chronic stroke: Implications for treatment. *NeuroImage: Clinical*, 36:103178, 2022.

[134] Daniel Gomes da Silva Machado, Marom Bikson, Abhishek Datta, Egas Caparelli-Dáquer, Gozde Unal, Abrahão F Baptista, Edilson Serpeloni Cyrino, Li Min Li, Edgard Morya, Alexandre Moreira, et al. Acute effect of high-definition and conventional tdcS on exercise performance and psychophysiological responses in endurance athletes: a randomized controlled trial. *Scientific Reports*, 11(1):1–15, 2021.

[135] Mia Kolmos, Mads Just Madsen, Marie Louise Liu, Anke Karabanov, Katrine Lyders Johansen, Axel Thielscher, Karen Gandrup, Henrik Lundell, Søren Fuglsang, Esben Thade, et al. Patient-tailored transcranial direct current stimulation to improve stroke rehabilitation: study protocol of a randomized sham-controlled trial. *Trials*, 24(1):216, 2023.

[136] Asad Khan, Marios Antonakakis, Sonja Suntrup-Krueger, Rebekka Lencer, Michael A Nitsche, Walter Paulus, Joachim Groß, and Carsten H Wolters. Can individually targeted and optimized multi-channel tdcS outperform standard bipolar tdcS in stimulating the primary somatosensory cortex? *Brain Stimulation*, 16(1):1–16, 2023.

[137] Mayank A Jog, Cole Anderson, Antoni Kubicki, Michael Boucher, Amber Leaver, Gerhard Hellemann, Marco Iacoboni, Roger Woods, and Katherine Narr. Transcranial direct current stimulation (tdcS) in depression induces structural plasticity. *Scientific reports*, 13(1):2841, 2023.

[138] Kevin A Caulfield, Aprinda Indahlastari, Nicole R Nissim, James W Lopez, Holly H Fleischmann, Adam J Woods, and Mark S George. Electric field strength from prefrontal transcranial direct current stimulation determines degree of working memory response: a potential application of reverse-calculation modeling? *Neuro-modulation: Technology at the Neural Interface*, 25(4):578–587, 2022.

[139] Daria Antonenko, Friederike Thams, Ulrike Grittner, Jessica Uhrich, Franka Glöckner, Shu-Chen Li, and Agnes Flöel. Randomized trial of cognitive training and brain stimulation in non-demented older adults. *Alzheimer's & Dementia: Translational Research & Clinical Interventions*, 8(1):e12262, 2022.

[140] Ghazaleh Soleimani, Rayus Kupliki, Jerzy Bodurka, Martin P Paulus, and Hamed Ekhtiari. How structural and functional mri can inform dual-site tacs parameters: A case study in a clinical population and its pragmatic implications. *Brain stimulation*, 15(2):337–351, 2022.

[141] Paulo JC Suen, Sarah Doll, Marcelo C Batistuzzo, Geraldo Busatto, Lais B Razza, Frank Padberg, Eva Mezger, Lucia Bulubas, Daniel Keeser, Zhi-De Deng, et al. Association between tdcS computational modeling and clinical outcomes in depression: data from the elect-tdcS trial. *European archives of psychiatry and clinical neuroscience*, 271:101–110, 2021.

[142] Toni Muffel, Franziska Kirsch, Pei-Cheng Shih, Benjamin Kalloch, Sara Schaumberg, Arno Villringer, and Bernhard Sehm. Anodal transcranial direct current stimulation over s1 differentially modulates proprioceptive accuracy in young and old adults. *Frontiers in aging neuroscience*, 11:264, 2019.

[143] Ajil Jalal, Marius Arvinte, Giannis Daras, Eric Price, Alexandros G Dimakis, and Jon Tamir. Robust compressed sensing mri with deep generative priors. *Advances in Neural Information Processing Systems*, 34:14938–14954, 2021.

[144] Konstantin Weise, William A Wartman, Thomas R Knösche, Aapo R Nummenmaa, and Sergey N Makarov. The effect of meninges on the electric fields in tes and tms. numerical modeling with adaptive mesh refinement. *Brain Stimulation*, 15(3):654–663, 2022.

[145] Heng Wang, Weiqian Sun, Jianxu Zhang, Zilong Yan, Chenyu Wang, Luyao Wang, Tiantian Liu, Chunlin Li, Duanduan Chen, Funahashi Shintaro, et al. Influence of layered skull modeling on the frequency sensitivity and target accuracy in simulations of transcranial current stimulation. *Human Brain Mapping*, 42(16):5345–5356, 2021.

[146] Ivana Despotović, Ewout Vansteenkiste, and Wilfried Philips. A realistic volume conductor model of the neonatal head: methods, challenges and applications. In *2013 35th Annual International Conference of the IEEE Engineering in Medicine and Biology Society (EMBC)*, pages 3303–3306. IEEE, 2013.

[147] Leslie A Geddes and Lee E Baker. The specific resistance of biological material—a compendium of data for the biomedical engineer and physiologist. *Medical and biological engineering*, 5:271–293, 1967.

[148] Andres Carvallo, Julien Modolo, Pascal Benquet, Stanislas Lagarde, Fabrice Bartolomei, and Fabrice Wendling. Biophysical modeling for brain tissue conductivity estimation using seeg electrodes. *IEEE Transactions on Biomedical Engineering*, 66(6):1695–1704, 2018.

[149] Guilherme B Saturnino, Axel Thielscher, Kristoffer H Madsen, Thomas R Knösche, and Konstantin Weise. A principled approach to conductivity uncertainty analysis in electric field calculations. *Neuroimage*, 188:821–834, 2019.

[150] David S. Tuch, Van J. Wedeen, Anders M. Dale, John S. George, and John W. Belliveau. Conductivity tensor mapping of the human brain using diffusion tensor mri. *Proceedings of the National Academy of Sciences of the United States of America*, 98:11697 – 11701, 2001.

[151] Alexander Opitz, Mirko Windhoff, Robin M. Heidemann, Robert Turner, and Axel Thielscher. How the brain tissue shapes the electric field induced by transcranial magnetic stimulation. *NeuroImage*, 58:849–859, 2011.

[152] Hyun Sang Suh, Won Hee Lee, and Tae-Seong Kim. Influence of anisotropic conductivity in the skull and white matter on transcranial direct current stimulation via an anatomically realistic finite element head model. *Physics in Medicine and Biology*, 57:6961 – 6980, 2012.

[153] Flavio Fröhlich and David A. McCormick. Endogenous electric fields may guide neocortical network activity. *Neuron*, 67:129–143, 2010.

[154] Yuhang Wang, Qiongfang Cao, Changyou Wei, Fan Xu, Peng Zhang, Hanrui Zeng, Yongcong Shao, Xiechuan Weng, and Rong Meng. The effect of transcranial electrical stimulation on the recovery of sleep quality after sleep deprivation based on an eeg analysis. *Brain Sciences*, 13, 2023.

[155] Syoichi Tashiro, Hartwig Roman Siebner, Angeliki Charalampaki, Cihan Göksu, Guilherme Bicalho Saturnino, Axel Thielscher, and Leo Tomasevic. Probing eeg activity in the targeted cortex after focal transcranial electrical stimulation. *Brain Stimulation*, 13:815–818, 2020.

[156] Beni Mulyana, Aki Tsuchiyagaito, Masaya Misaki, Rayus Kuplicki, Jared Smith, Ghazaleh Soleimani, Ashkan Rashedi, Duke Shereen, Til Ole Bergman, Samuel Cheng, Martin P. Paulus, Jerzy Bodurka, and Hamed Ekhtiari. Online closed-loop real-time tes-fmri for brain modulation: A technical report. *Brain and Behavior*, 12, 2022.

[157] Peyman Ghobadi-Azbari, Asif Jamil, Fatemeh Yavari, Zeinab Esmaeilpour, Nastaran Malmir, Rasoul Mahdavifar-Khayati, Ghazaleh Soleimani, Yoon-Hee Cha, A. Duke Shereen, Michael A. Nitsche, Marom Bikson, and Hamed Ekhtiari. fmri and transcranial electrical stimulation (tes): A systematic review of parameter space and outcomes. *Progress in Neuro-Psychopharmacology and Biological Psychiatry*, 107, 2020.

[158] Beni Mulyana, Aki Tsuchiyagaito, Jared Smith, Masaya Misaki, Rayus Kuplicki, Ghazaleh Soleimani, Ashkan Rashedi, Duke Shereen, Til Ole Bergman, Samuel Cheng, Martin P. Paulus, Jerzy Bodurka, and Hamed Ekhtiari. Online closed-loop real-time tes-fmri for brain modulation: Feasibility, noise/safety and pilot study. *bioRxiv*, 2021.

[159] Samuel Louvion, Louise Tyvaert, Louis G Maillard, Sophie Colnat-Coulbois, Jacek Dmochowski, and Laurent Koessler. Transcranial electrical stimulation generates electric fields in deep human brain structures. *Brain Stimulation*, 15(1):1–12, 2022.

[160] Kexin Lou, Jingzhe Li, Markus Barth, and Quanying Liu. A data-driven framework for whole-brain network modeling with simultaneous eeg-seeg data. In *Intelligent Information Processing*, 2024.

[161] Giulio Ruffini, Michael D. Fox, Oscar Ripolles, Pedro Cavaleiro Miranda, and Álvaro Pascual-Leone. Optimization of multifocal transcranial current stimulation for weighted cortical pattern targeting from realistic modeling of electric fields. *NeuroImage*, 89:216–225, 2014.

[162] Mohsin Ali, Kristin K. Sellers, and Flavio Fröhlich. Transcranial alternating current stimulation modulates large-scale cortical network activity by network resonance. *The Journal of Neuroscience*, 33:11262 – 11275, 2013.

[163] Reza Rostami, Reza Kazemi, Farzaneh Mozaffarinejad, Zahra Nasiri, Maryam Rostami, Abed L.Hadipour, and Fatemeh Sadeghiahassanabadi. 6 hz transcranial alternating current stimulation of mpfc improves sustained attention and modulates alpha phase synchronization and power in dorsal attention network. *Cognitive Neuroscience*, 12:1 – 13, 2020.

[164] Matthew R. Krause, Pedro G. Vieira, Bennett A. Csorba, Praveen K. Pilly, and Christopher C. Pack. Transcranial alternating current stimulation entrains single-neuron activity in the primate brain. *Proceedings of the National Academy of Sciences*, 116:5747 – 5755, 2019.

[165] Florian H. Kasten and Christoph Siegfried Herrmann. The hidden brain-state dynamics of tacs aftereffects. *NeuroImage*, 264, 2022.

[166] Joshua A. Brown, Kevin J. Clancy, Chaowen Chen, Yimeng Zeng, Shaozheng Qin, Mingzhou Ding, and Wen Li. Transcranial stimulation of alpha oscillations modulates brain state dynamics in sustained attention. *bioRxiv*, 2023.

[167] Shi Gu, Fabio Pasqualetti, Matthew Cieslak, Qawi K Telesford, Alfred B Yu, Ari E Kahn, John D Medaglia, Jean M Vettel, Michael B Miller, Scott T Grafton, et al. Controllability of structural brain networks. *Nature communications*, 6(1):8414, 2015.

[168] Jacob Tanner, Joshua Faskowitz, Andreia Sofia Teixeira, Caio Seguin, Ludovico Coletta, Alessandro Gozzi, Bratislav Mišić, and Richard F Betzel. A multi-modal, asymmetric, weighted, and signed description of anatomical connectivity. *Nature communications*, 15(1):5865, 2024.

[169] Zixiang Luo, Kaining Peng, Zhichao Liang, Shengyuan Cai, Chenyu Xu, Dan Li, Yu Hu, Changsong Zhou, and Quanying Liu. Mapping effective connectivity by virtually perturbing a surrogate brain. *Nature Methods*, pages 1–10, 2025.

[170] Meenakshi B Iyer, U Mattu, Jordan Grafman, Mikhail Lomarev, S Sato, and Eric M Wassermann. Safety and cognitive effect of frontal dc brain polarization in healthy individuals. *Neurology*, 64(5):872–875, 2005.

[171] Tommy Clausner, Sarang S. Dalal, and Maite Crespo-Garcia. Photogrammetry-based head digitization for rapid and accurate localization of eeg electrodes and meg fiducial markers using a single digital slr camera. *Frontiers in Neuroscience*, 11, 2017.

[172] Sagi Jaffe-Dax, Amit H. Bermano, Yotam Erel, and Lauren L. Emberson. Video-based motion-resilient reconstruction of 3d position for fnirs/eeg head mounted probes. *bioRxiv*, 2019.

[173] Quanying Liu, Chen Wei, Youzhi Qu, and Zhichao Liang. Modelling and controlling system dynamics of the brain: An intersection of machine learning and control theory. *Systems Neuroscience*, pages 63–87, 2024.

[174] Zhichao Liang, Zixiang Luo, Keyin Liu, Jingwei Qiu, and Quanying Liu. Online learning koopman operator for closed-loop electrical neurostimulation in epilepsy. *IEEE Journal of Biomedical and Health Informatics*, 27(1):492–503, 2022.

[175] Miguel Angel Lopez-Gordo, Daniel Sanchez-Morillo, and F Pelayo Valle. Dry eeg electrodes. *Sensors*, 14(7):12847–12870, 2014.

[176] Chuen Rue Ng, Patrique Fiedler, Levin Kuhlmann, David Liley, Beatriz Vasconcelos, Carlos Fonseca, Gabriella Tamburro, Silvia Comani, Troby Ka-Yan Lui, Chun-Yu Tse, et al. Multi-center evaluation of gel-based and dry multipin eeg caps. *Sensors*, 22(20):8079, 2022.

- [177] Nima Noury and Markus Siegel. Phase properties of transcranial electrical stimulation artifacts in electrophysiological recordings. *Neuroimage*, 158:406–416, 2017.
- [178] Nima Noury, Joerg F Hipp, and Markus Siegel. Physiological processes non-linearly affect electrophysiological recordings during transcranial electric stimulation. *Neuroimage*, 140:99–109, 2016.
- [179] David Haslacher, Khaled Nasr, Stephen E Robinson, Christoph Braun, and Surjo R Soekadar. Stimulation artifact source separation (sass) for assessing electric brain oscillations during transcranial alternating current stimulation (tacs). *Neuroimage*, 228:117571, 2021.
- [180] Siddharth Kohli and Alexander J Casson. Removal of transcranial ac current stimulation artifact from simultaneous eeg recordings by superposition of moving averages. In *2015 37th Annual International Conference of the IEEE Engineering in Medicine and Biology Society (EMBC)*, pages 3436–3439. IEEE, 2015.
- [181] Johannes Voskuhl, Tuomas P Mutanen, Toralf Neuling, Risto J Ilmoniemi, and Christoph S Herrmann. Signal-space projection suppresses the tacs artifact in eeg recordings. *Frontiers in Human Neuroscience*, 14:536070, 2020.
- [182] Roberto Guarneri, Alfredo Brancucci, Anita D’Anselmo, Valerio Manippa, Stephan P Swinnen, Franca Tecchio, and Dante Mantini. A computationally efficient method for the attenuation of alternating current stimulation artifacts in electroencephalographic recordings. *Journal of neural engineering*, 17(4):046038, 2020.
- [183] Siddharth Kohli and Alexander J Casson. Machine learning validation of eeg+ tacs artefact removal. *Journal of neural engineering*, 17(1):016034, 2020.
- [184] Ruobing Liu, Guanyu Zhu, Zhengping Wu, Yifei Gan, Jianguo Zhang, Jiali Liu, and Liang Wang. Temporal interference stimulation targets deep primate brain. *NeuroImage*, 291, 2024.
- [185] Camelia Gabriel, Serban Mihai Gabriel, and Erik Corthout. The dielectric properties of biological tissues: I. literature survey. *Physics in medicine and biology*, 41 11:2231–49, 1996.
- [186] Bruce Hutcheon and Yosef Yarom. Resonance, oscillation and the intrinsic frequency preferences of neurons. *Trends in neurosciences*, 23(5):216–222, 2000.